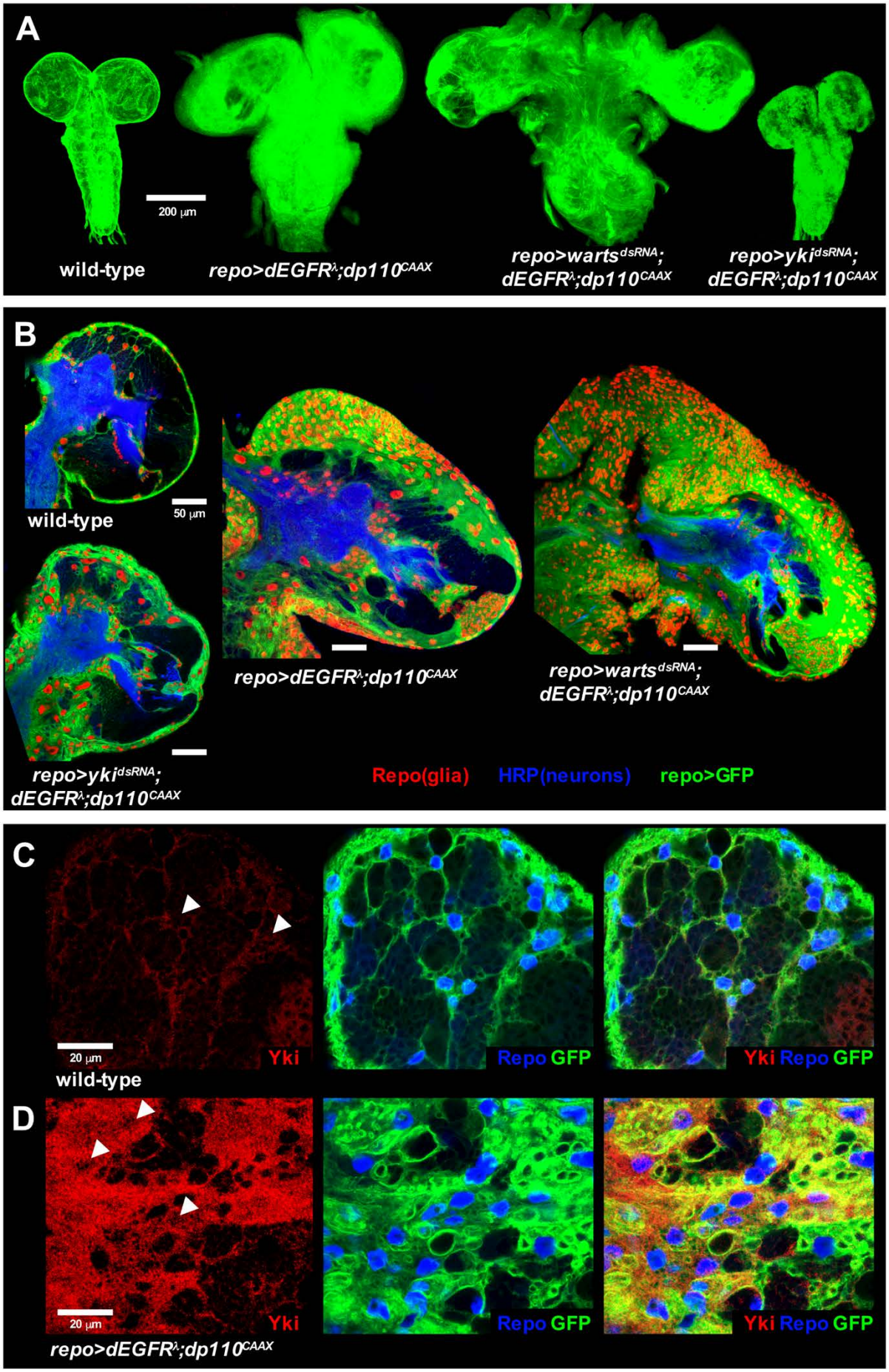
A
200 μm
wild-type
repo>dEGFR$^{\lambda}$;dp110^{CAAX}
repo>warts^{dsRNA}; dEGFR$^{\lambda}$;dp110^{CAAX}
repo>yki^{dsRNA}; dEGFR$^{\lambda}$;dp110^{CAAX}
B
50 μm
wild-type
repo>dEGFR$^{\lambda}$;dp110^{CAAX}
repo>warts^{dsRNA}; dEGFR$^{\lambda}$;dp110^{CAAX}
repo>yki^{dsRNA}; dEGFR$^{\lambda}$;dp110^{CAAX}
Repo(glia) HRP(neurons) repo>GFP
C
20 μm
Yki
Repo GFP
Yki Repo GFP
wild-type
D
20 μm
Yki
Repo GFP
Yki Repo GFP
repo>dEGFR$^{\lambda}$;dp110^{CAAX}

Figure S1: Yki is required for EGFR-PI3K-driven glial neoplasia in *Drosophila*

(A) Optical projections of whole brain-nerve cord complexes from 3rd instar larvae approximately 130 hrs old. Dorsal view; anterior up. CD8-GFP (green) labels glial cell bodies. Compared to *repo>dEGFR$^{\lambda}$;dp110^{CAAX}*, *warts* knockdown (*repo>warts^{dsRNA}; dEGFR$^{\lambda}$;dp110^{CAAX}*) increased neoplastic brain overgrowth and *yki* knockdown (*repo>yki^{dsRNA};dEGFR$^{\lambda}$;dp110^{CAAX}*) decreased neoplastic brain overgrowth.
(B) 3 µm optical projections of brain hemispheres, age-matched 3rd instar larvae. Frontal sections; anterior up; midline to left. Repo (red) labels glial cell nuclei; CD8-GFP (green) labels glial cell bodies; anti-HRP (blue) counter-stains for neurons and neuropil. (middle) *repo>dEGFR$^{\lambda}$;dp110^{CAAX}* showed increased glial cell numbers (red nuclei) compared to (upper left) wild-type. Compared to *repo>dEGFR$^{\lambda}$;dp110^{CAAX}*, (right) *warts* knockdown increased neoplastic glial cell numbers (red nuclei), whereas (lower left) *yki* knockdown reduced neoplastic glial cell numbers (red nuclei).
(C, D) Low levels of Yki protein (red) was observed in wild-type central brain glia (white arrows, left panel in **C**) compared to high levels of cytoplasmic and nuclear Yki protein in *dEGFR$^{\lambda}$;dp110^{CAAX}* neoplastic glia (white arrows, left panel in **D**); Repo (blue) labels glial cell nuclei; CD8-GFP (green) labels glial cell bodies.

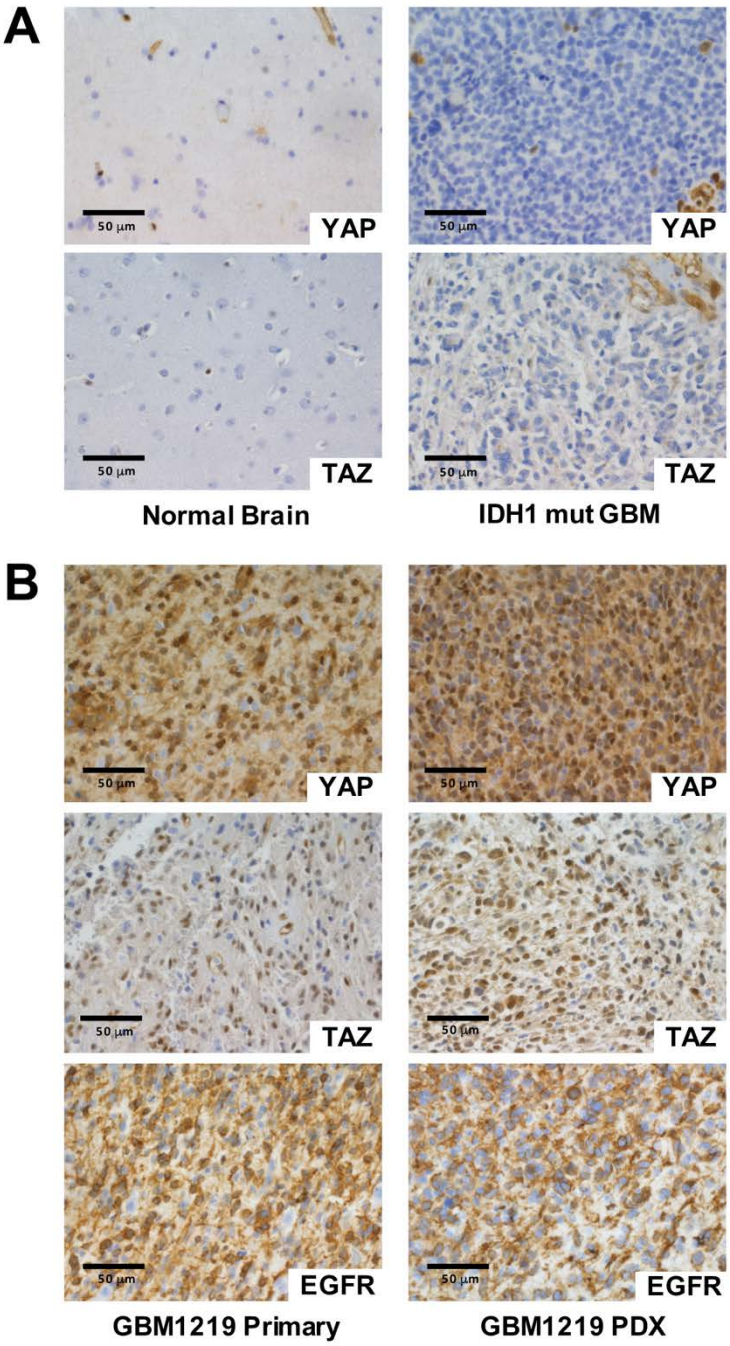

Figure S2: YAP/TAZ expression confined to RTK-amplified tumor cells and maintained in patient-derived xenografts

(A) On the left, immunohistochemical (IHC) staining in representative normal brain parenchyma in the cortex where YAP expression and TAZ expression was limited to vascular cells and was not detectable in normal neuronal and glial cells. On the right, IHC staining in a representative IHD1-mutant GBM specimen showed YAP and TAZ expression was detectable in vascular cells, but was present at low or undetectable levels in tumor cells.
(B) IHC for YAP, TAZ, and EGFR expression in tissue from an EGFR-amplified GBM tumor specimen and its matched patient-derived orthotopic xenograft. YAP and TAZ staining show cytoplasmic and nuclear localization (overlap with nuclear counterstain).

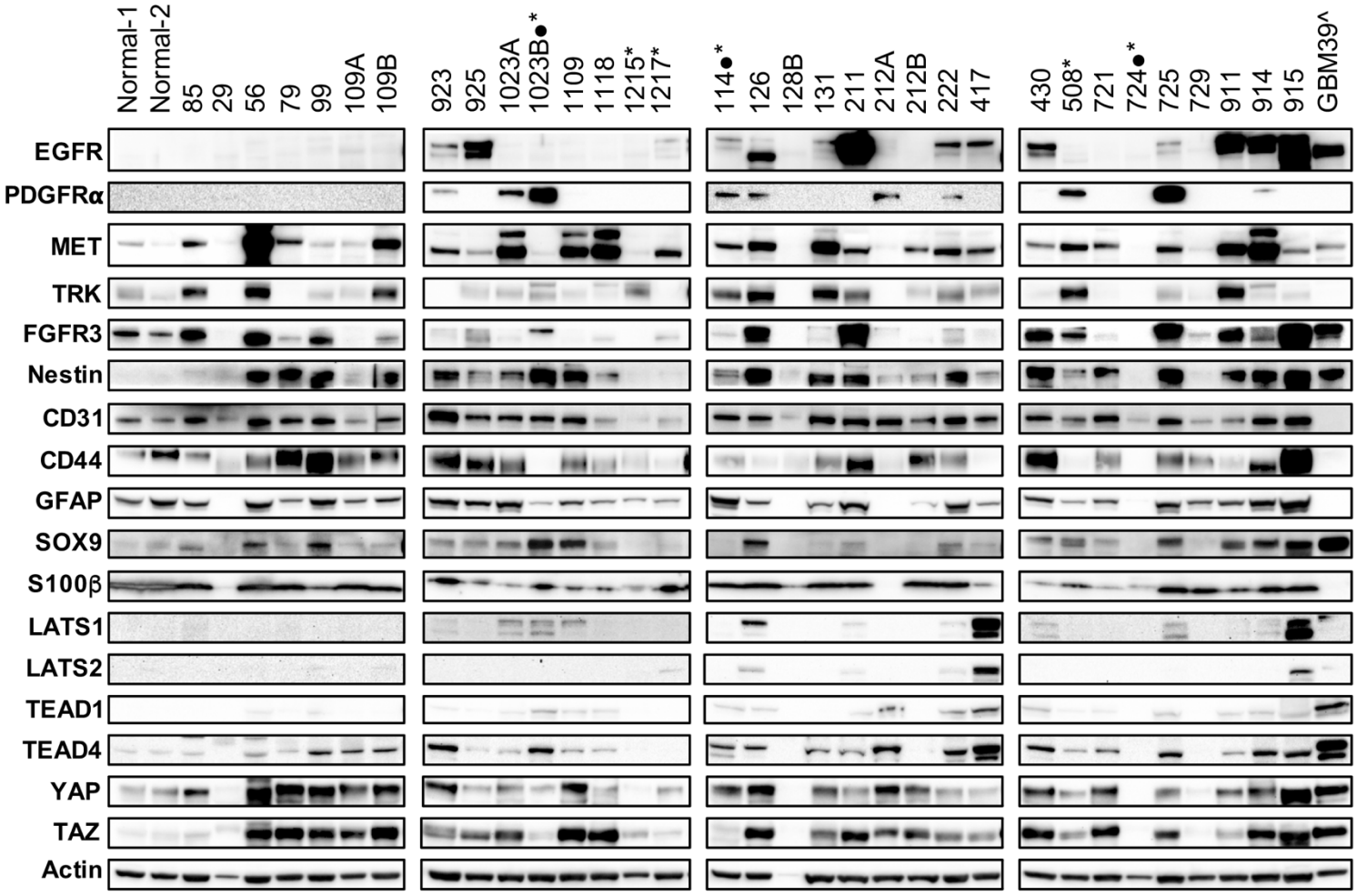

Figure S3: YAP and TAZ are co-overexpressed in GBM

Total tissue lysates from GBM surgical specimens immunoblotted for the indicated proteins. (●) indicates tumors with IDH1 mutations. (*) indicates tumors with low YAP and TAZ expression by IHC. (^) indicates GBM39 GSC neurosphere culture as a control for tumor-cell specific protein expression. High Nestin expression (stem cell marker) indicates specimens that contain mainly tumor. Lower migrating forms of EGFR (925, 126, 211, 430, and 915) are likely to be mutant variants such as $EGFR^{vIII}$ (as in GBM39). The majority of GBM tumor specimens showed co-overexpression of YAP, TAZ, and TEAD4, and these tumors typically expressed markers that are predominantly associated with the classical (CL) subtype of adult GBM, such as EGFR, EGFR variants, other RTKs, such as FGFR3, and astrocytic markers GFAP, SOX9, and S100β. GBM tumor specimens that predominantly expressed indicators of the mesenchymal (MES) subtype (MET, CD44) also expressed TAZ, as previously published. GBM tumor specimens from IDH1 mutant (●) tumors showed low YAP and TAZ expression comparable with normal brain control tissue specimens.

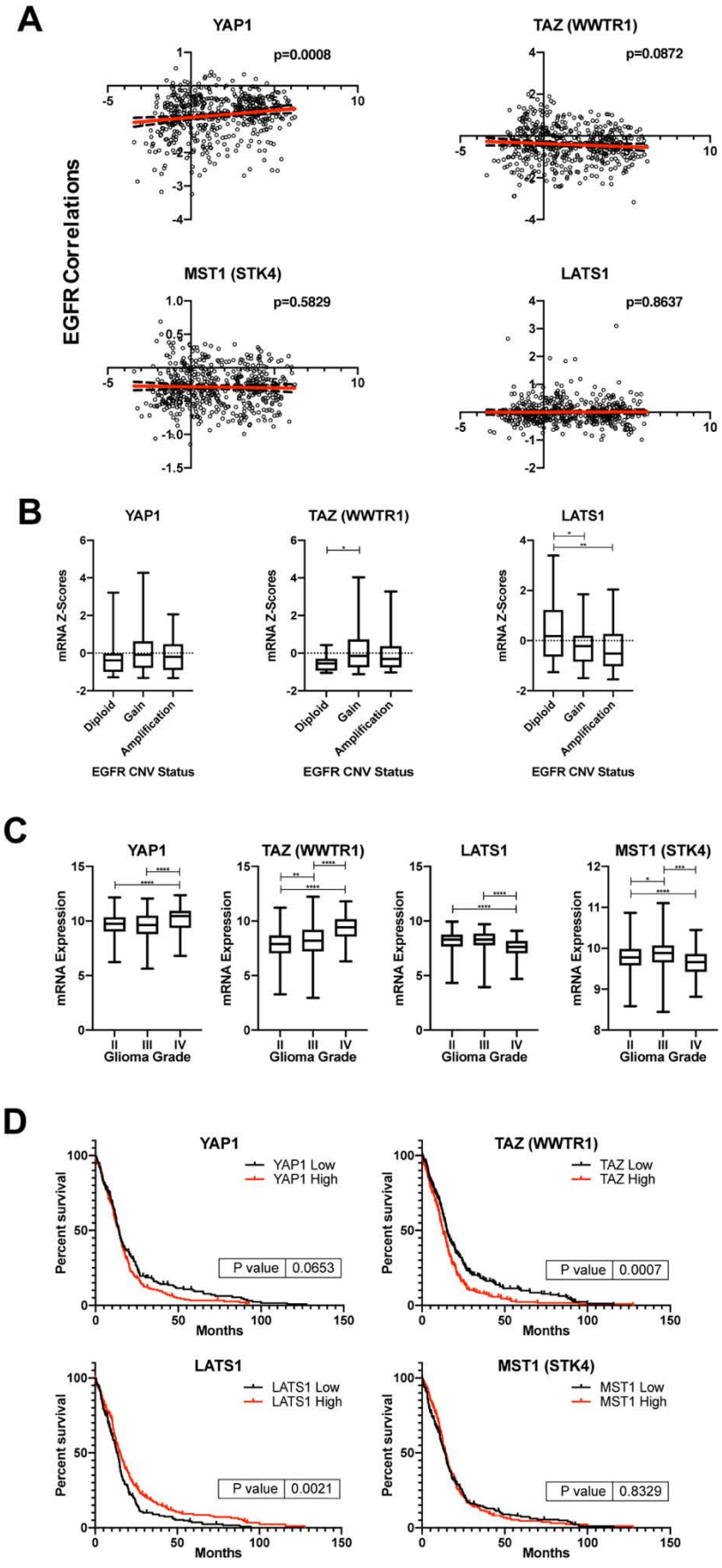
A
YAP1
p=0.0008
TAZ (WWTR1)
p=0.0872
MST1 (STK4)
p=0.5829
LATS1
p=0.8637
EGFR Correlations
B
YAP1
TAZ (WWTR1)
LATS1
mRNA Z-Scores
Diploid
Gain
Amplification
EGFR CNV Status
C
YAP1
TAZ (WWTR1)
LATS1
MST1 (STK4)
mRNA Expression
II
III
IV
Glioma Grade
D
YAP1
YAP1 Low
YAP1 High
P value 0.0653
TAZ (WWTR1)
TAZ Low
TAZ High
P value 0.0007
LATS1
LATS1 Low
LATS1 High
P value 0.0021
MST1 (STK4)
MST1 Low
MST1 High
P value 0.8329
Percent survival
Months

Figure S4: Hippo pathway kinases are implicated in high tumor grade, poor survival, and associated with RTK overexpression

(A) Correlation of mRNA expression of Hippo pathway member kinases with *EGFR* mRNA expression in GBM patients in the Cancer Genome Atlas database. *YAP1*(YAP) mRNA expression is positively and significantly correlated with *EGFR* mRNA expression. Other pathway members had a non-significant correlation with *EGFR* mRNA expression. Reported p-value was generated using Fisher's statistical test.
(B) *YAP1*, *TAZ*, and *LATS1* mRNA expression segregated by GBM tumors with *EGFR* copy number variants. *TAZ* expression is significantly increased in GBM tumors with *EGFR* copy number gain. YAP/TAZ regulator *LATS1* expression is significantly decreased in tumors with *EGFR* copy number gain. *, $p < .05$; **, $p < .01$; ***, $p < .001$; ****, $p < .0001$ with ANOVA multiple comparisons test.
(C) mRNA expression scores for *YAP1* and *TAZ* and the YAP/TAZ regulators *LATS1* and *MST1* in higher glioma grades. mRNA expression data from The Cancer Genome Atlas was accessed and downloaded with GlioVis. *, $p < .05$; **, $p < .01$; ***, $p < .001$; ****, $p < .0001$ with ANOVA multiple comparisons test.
(D) mRNA expression data from Hippo pathway members as correlated by GBM patient survival in the Cancer Genome Atlas. Higher *YAP1/TAZ* mRNA expression associates with worse GBM patient survival whereas high expression of YAP/TAZ regulator *LATS1* is associated with better survival in GBM patients. There was no difference in *MST1* mRNA expression related to patient survival in GBM. This data was accessed and downloaded using GlioVis and segregated into low and high mRNA expression using the median expression level as a cutoff. Reported p-value was generated using Log-rank (Mantel-Cox) statistical test.

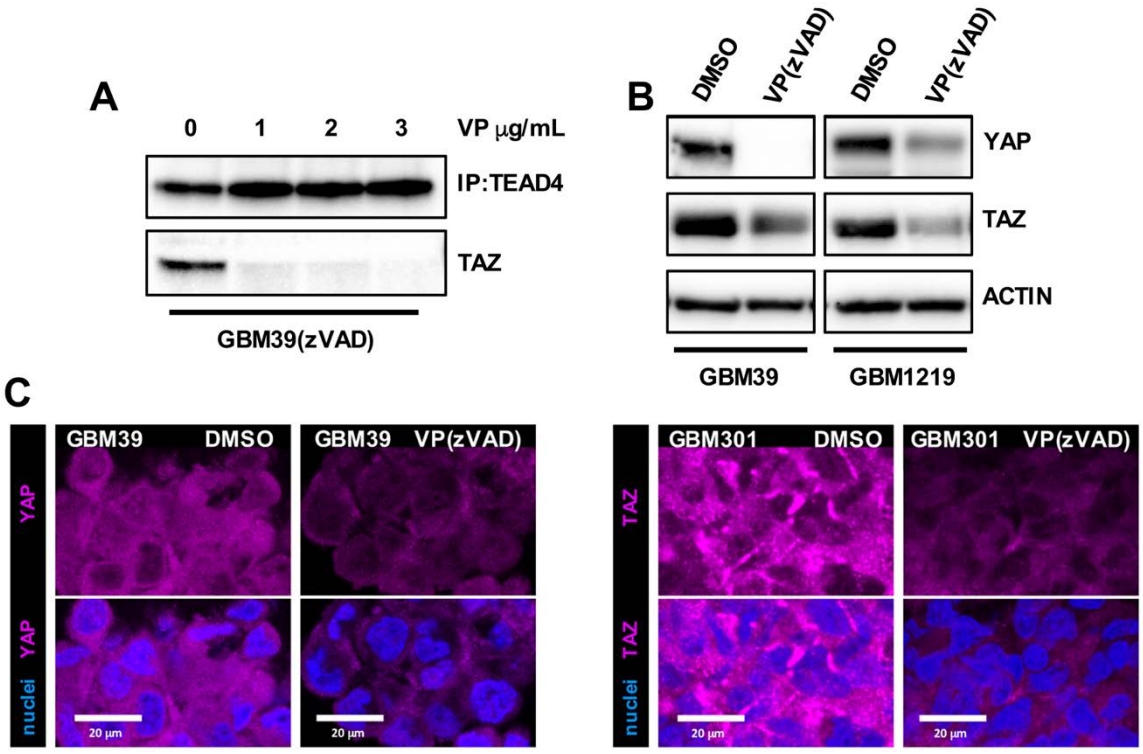

Figure S5: YAP and TAZ function is disrupted by Verteporfin (VP)

(A) GBM39 cells expressing TAZ were incubated with the indicated concentrations of VP combined with 20 μM zVAD for 8 hours, subject to lysis and anti-TEAD4 immuno-precipitation, and the presence of TAZ in TEAD4 immunoprecipitates was probed by immunoblot. VP-mediated inhibition of TAZ-TEAD4 interaction was detected with drug doses of 1 μg/mL and higher.
(B, C) (B) GBM39 and GBM1219 cells treated with 1 μg/mL VP for 24 hrs. **(C)** GBM39 and GBM301 cells treated with .5 μg/mL VP for 24 hrs; 20 μM zVAD was included to block secondary changes caused by apoptosis. 2.5 μm confocal optical sections of whole mount neurospheres stained for YAP or TAZ (magenta) and for all nuclei (DRAQ7, blue). Total YAP and TAZ protein levels declined with VP treatment in the presence of zVAD, as detected by immunoblots and confocal imaging of GSCs, with reduced YAP and TAZ nuclear localization in GSCs.

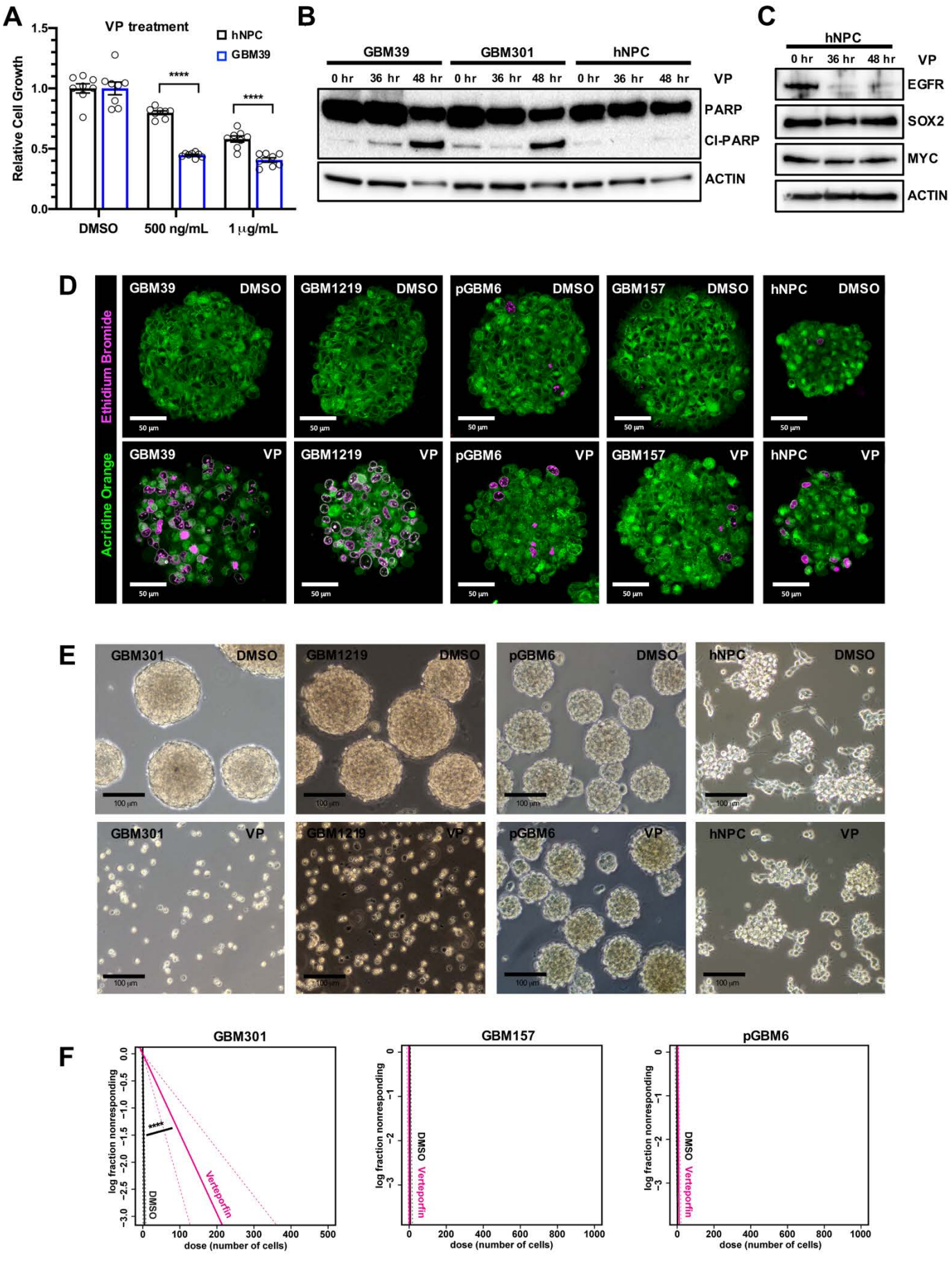
A
VP treatment
hNPC
GBM39
Relative Cell Growth
1.5
1.0
0.5
0.0
****
****
DMSO
500 ng/mL
1 μg/mL
B
GBM39
GBM301
hNPC
0 hr
36 hr
48 hr
VP
PARP
Cl-PARP
ACTIN
C
hNPC
0 hr
36 hr
48 hr
VP
EGFR
SOX2
MYC
ACTIN
D
Ethidium Bromide
Acridine Orange
GBM39 DMSO
GBM1219 DMSO
pGBM6 DMSO
GBM157 DMSO
hNPC DMSO
GBM39 VP
GBM1219 VP
pGBM6 VP
GBM157 VP
hNPC VP
50 μm
E
GBM301 DMSO
GBM1219 DMSO
pGBM6 DMSO
hNPC DMSO
GBM301 VP
GBM1219 VP
pGBM6 VP
hNPC VP
100 μm
F
GBM301
GBM157
pGBM6
log fraction nonresponding
dose (number of cells)
DMSO
Verteporfin
****

Figure S6: Verteporfin preferentially targets GBM stem cells

(A) hNPCs (black bars) and GBM39 (blue bars) were treated with the indicated concentrations of VP for 48 hours and observed for cell growth/viability via WST-1 assay. All replicates are indicated individually as circle icons for each bar representing each cell type and condition. Statistical comparisons made between the effects of DMSO and VP on GBM39 and hNPCs, **** $p < .0001$ with multi two-stage two-tailed t-tests.
(B) Cultured GBM39 and GBM301 GSCs and hNPCs were incubated with 1 μg/mL VP for 36 and 48 hours, harvested for protein lysates, and examined by immunoblot for PARP protein to assess apoptosis; the presence of cleaved PARP (Cl-PARP) indicates apoptosis.
(C) Protein expression of EGFR, SOX2, and MYC in hNPCs neurospheres following VP treatment for 36 and 48 hours. Non-adherently cultured cells were treated with 1 μg/mL VP and harvested at the indicated timepoints for protein.
(D) Representative images from established GSC and hNPC neurosphere cultures treated with .5 μg/mL of VP for 24 hours. Apoptosis was visualized by ethidium bromide (magenta) dye exclusion assays. Acridine orange (green) used to counterstain cell bodies. 3 μm confocal optical projections.
(E) Established GBM301 and GBM1219 GSCs treated with VP for 3 days to determine the gross effect of VP on neurosphere survival and growth as compared to YAP/TAZ-negative pGBM6 GSCs and control hNPC neurospheres. GBM301, GBM1219, and hNPCs cells were treated with 1 μg/mL VP or DMSO as a control, and pGBM6 cells were treated with 3 μg/mL VP or DMSO as a control.
(F) Limiting dilution assays in which GSCs and hNPCs were plated at low density of 1-1000 cells per well in 96 well plates, incubated with 1 μg/mL VP, and observed for neurosphere formation after 7 days. **** $p < .0001$ with chi-squared test.

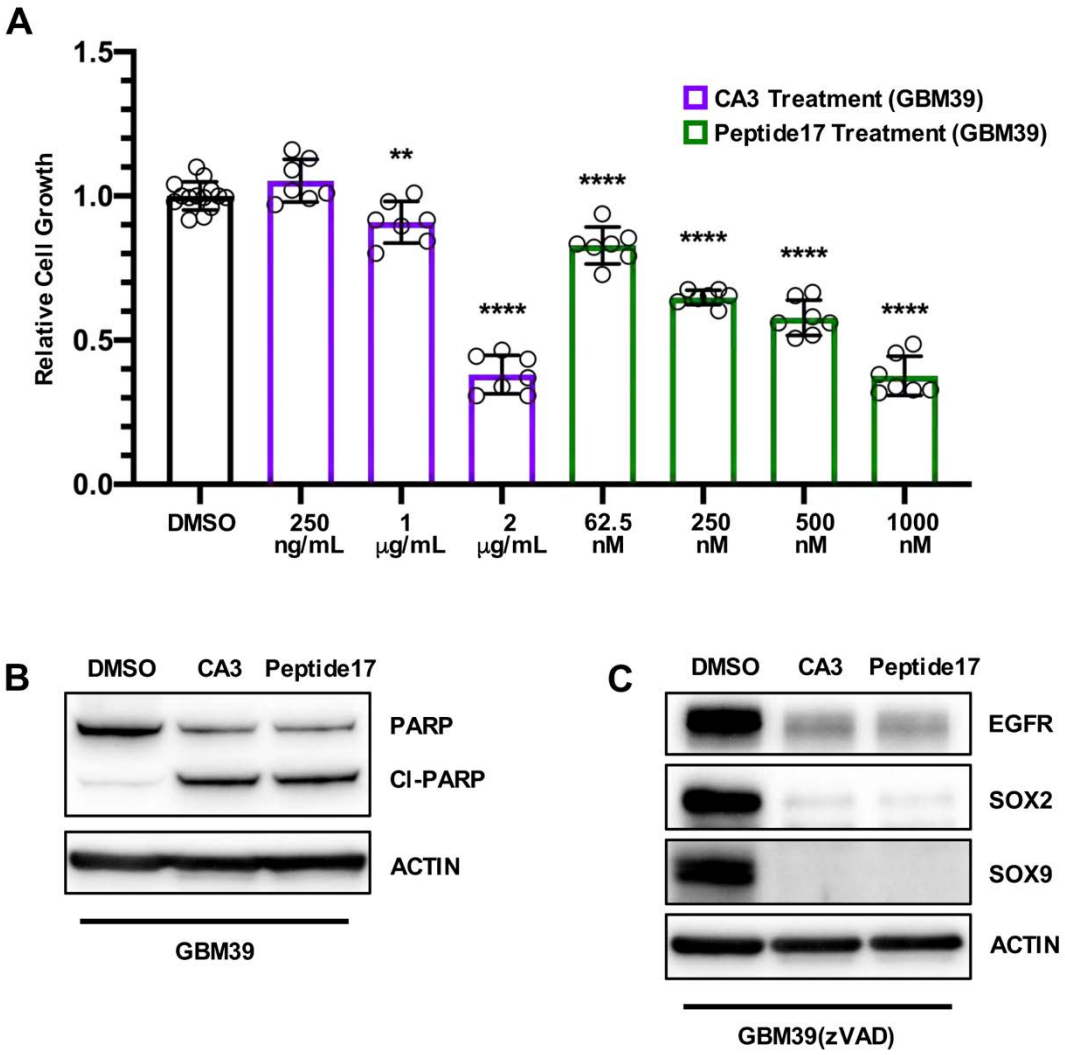

Figure S7: Alternate YAP/TAZ-TEAD inhibitors target GBM cell survival and reduce stem cell gene expression

(A) CA3 and Peptide17, which are small molecule inhibitors of the interaction between YAP and TAZ and the TEADs, were tested to determine if they affect GMB39 cell growth and viability in a dose-dependent manner. GBM39 GSCs were incubated with indicated concentrations of CA3 or Peptide17 for 48 hours and observed for growth/viability via WST-1 assay. For comparison, these assays were run alongside VP WST-1 assays shown in Figure 3B, so both plots shown here use the same set of DMSO treated control samples as a result. ** p<.01; *** p<.001; **** p<.0001 with multi two-tailed t-tests.
(B) Immunoblot for PARP cleavage (Cl-PARP) to assess apoptosis in GBM39 GSCs following treatment with DMSO, 1 μg/mL CA3, or 500 nM Peptide17 treatment for 24 hours.
(C) EGFR, SOX2, and SOX9 protein expression of in GBM39 GSCs following treatment with DMSO, 1 μg/mL CA3, or 500 nM Peptide17 treatment for 24 hours, 20 μm zVAD used to prevent apoptosis and preserve signaling pathways.

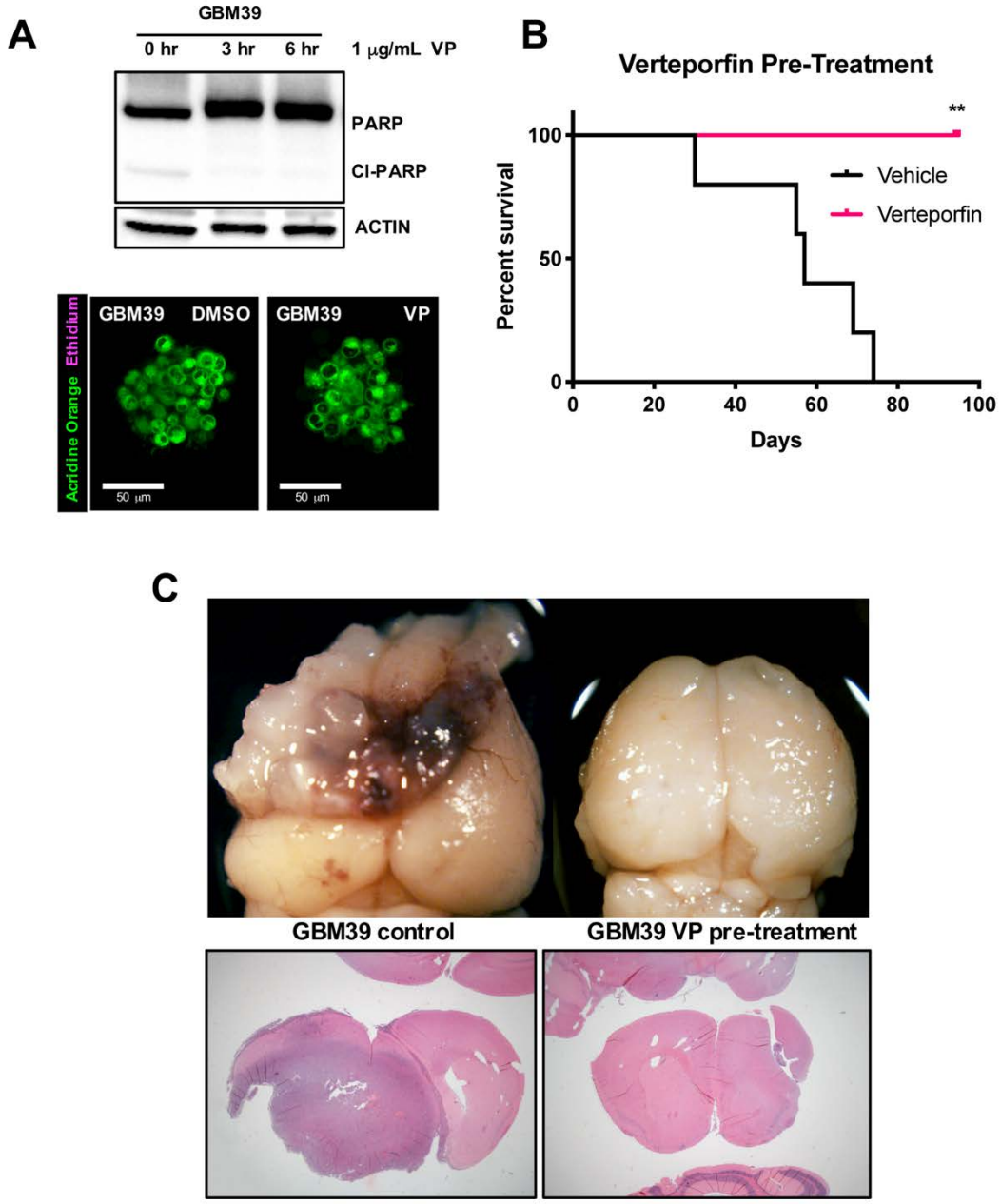

Figure S8: Short-term pre-treatment of GSCs with Verteporfin reduces their tumorigenicity

(A) GBM39 GSCs treated with 1 μg/mL VP for 3 and 6 hours. Apoptosis was assessed by immunoblotting for PARP cleavage and by ethidium bromide absorption in dye exclusion assays. 3 μm confocal optical sections.
(B) Kaplan-Meier curve showing survival of NSG mice orthotopically implanted GBM39 GSCs pre-treated with 1 μg/mL VP or DMSO (vehicle control) for 4-6 hours. ** $p < .01$ with Log-rank (Mantel-Cox) test (n=5 for each treatment group).
(C) Representative photos and H&E stains are depicted of brains from animals implanted with DMSO (vehicle control) or VP-treated GSCs.

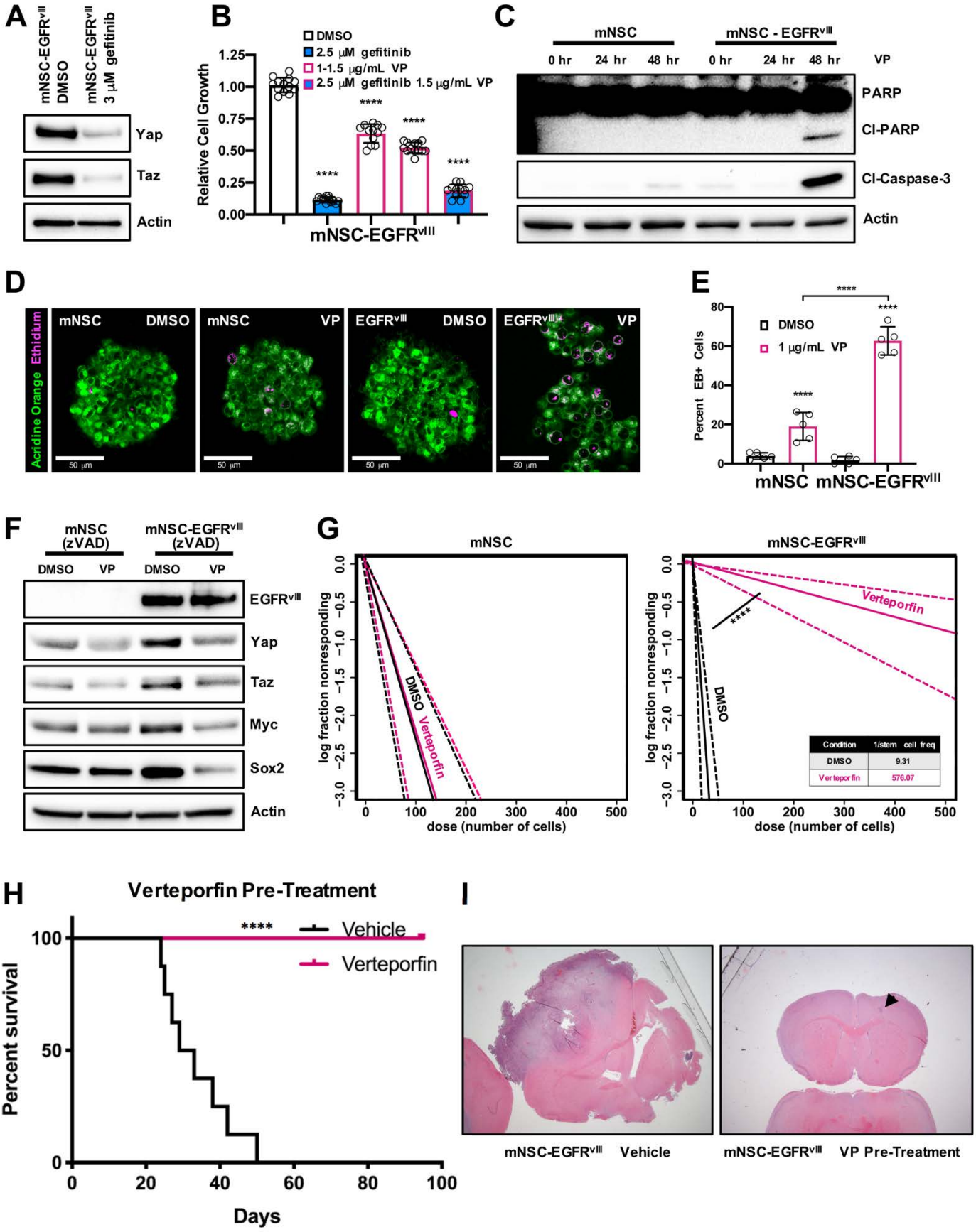
A
mNSC-EGFRvIII DMSO
mNSC-EGFRvIII 3 μM gefitinib
Yap
Taz
Actin
B
DMSO
2.5 μM gefitinib
1-1.5 μg/mL VP
2.5 μM gefitinib 1.5 μg/mL VP
Relative Cell Growth
mNSC-EGFRvIII
C
mNSC
mNSC - EGFRvIII
0 hr 24 hr 48 hr 0 hr 24 hr 48 hr VP
PARP
Cl-PARP
Cl-Caspase-3
Actin
D
Acridine Orange Ethidium
mNSC DMSO
mNSC VP
EGFRvIII DMSO
EGFRvIII VP
50 μm
E
DMSO
1 μg/mL VP
Percent EB+ Cells
mNSC mNSC-EGFRvIII
F
mNSC (zVAD)
mNSC-EGFRvIII (zVAD)
DMSO VP DMSO VP
EGFRvIII
Yap
Taz
Myc
Sox2
Actin
G
mNSC
mNSC-EGFRvIII
log fraction nonresponding
dose (number of cells)
DMSO
Verteporfin
Condition 1/stem cell freq
DMSO 9.31
Verteporfin 576.07
H
Verteporfin Pre-Treatment
Vehicle
Verteporfin
Percent survival
Days
I
mNSC-EGFRvIII Vehicle
mNSC-EGFRvIII VP Pre-Treatment

Figure S9: EGFR^{vIII} transformed mNSCs are sensitive to Verteporfin

(A) *EGFR^{vIII}; Cdkn2a$^{-/-}$; Pten$^{-/-}$* mNSC neurospheres treated with DMSO or 2.5 μM/mL gefitinib for 24 hours, and then harvested for immunoblots to determine if EGFR kinase inhibition affected Yap and Taz protein levels.
(B) WST-1 assay on *EGFR^{vIII}; Cdkn2a$^{-/-}$; Pten$^{-/-}$* mNSCs to examine their viability and growth in response to gefitinib and VP alone or combined. mNSCs were treated with DMSO as a control, VP at the indicated dose for 24 hrs, or with 2.5 μM gefitinib alone for 48 hours. Combination treatment involved 2.5 μM gefitinib for 24 hours followed by another 24 hrs of both 2.5 μM gefitinib and 1 μg/mL VP: this sequential design was meant to determine whether EGFR kinase inhibition rescued cells from VP or if VP had off-target effects distinct from EGFR inhibition. **** $p < .0001$ with one-way ANOVA relative to DMSO control.
(C) *EGFR^{vIII}; Cdkn2a$^{-/-}$; Pten$^{-/-}$* and control *Cdkn2a$^{-/-}$; Pten$^{-/-}$* mNSC neurosphere cultures were incubated with 1 μg/mL VP for 24 and 48 hours, harvested for protein lysates, and assessed for apoptosis by immunoblot for cleaved-Caspase-3 (Cl-Caspase-3) and cleaved PARP (Cl-PARP).
(D, E) Representative images from *EGFR^{vIII}; Cdkn2a$^{-/-}$; Pten$^{-/-}$* mNSCs and *Cdkn2a$^{-/-}$; Pten$^{-/-}$* mNSC neurosphere cultures treated with 1 μg/mL of VP for 24 hours. Apoptosis was visualized by ethidium bromide (magenta) dye exclusion assays. Acridine orange (green) used to counterstain cell bodies. 3 μm confocal optical projections. Graphs show the percentage of ethidium bromide-positive cells in the indicated mNSC cultures, counted in 25 μm optical projections. **** $p < .0001$ with ANOVA multiple comparisons test.
(F) Yap, Taz, EGFR^{vIII}, and tumor stem cell marker (Myc, Sox2) protein expression levels in the indicated mNSCs treated with 1 μg/mL VP or DMSO as a control for 24 hour; ZVAD (20 μM) was used to prevent the effects of apoptosis.
(G) Limiting dilution assay in which *EGFR^{vIII}; Cdkn2a$^{-/-}$; Pten$^{-/-}$* mNSCs and *Cdkn2a$^{-/-}$; Pten$^{-/-}$* mNSCs were plated at low density of 1-500 cells per well in 96 well plates, incubated with 1.5 μg/mL VP, and observed for neurosphere formation after 5 days. **** $p < .01$ with chi-squared test.
(H) Kaplan-Meier curve showing survival of NSG mice orthotopically implanted with *EGFR^{vIII}; Cdkn2a$^{-/-}$; Pten$^{-/-}$* mNSCs pre-treated with 1 μg/mL VP or DMSO (vehicle control) for 4-6 hours (n=9 for VP treatment, n=8 for controls). **** $p < .0001$ with log-rank (Mantel-Cox) test.
(I) Representative photos and H&E stains are depicted of brains from animals implanted with DMSO (vehicle control) and VP-treated *EGFR^{vIII}; Cdkn2a$^{-/-}$; Pten$^{-/-}$*mNSCs. Arrow indicates gliosis and likely needle scar in the pictured vehicle control section.

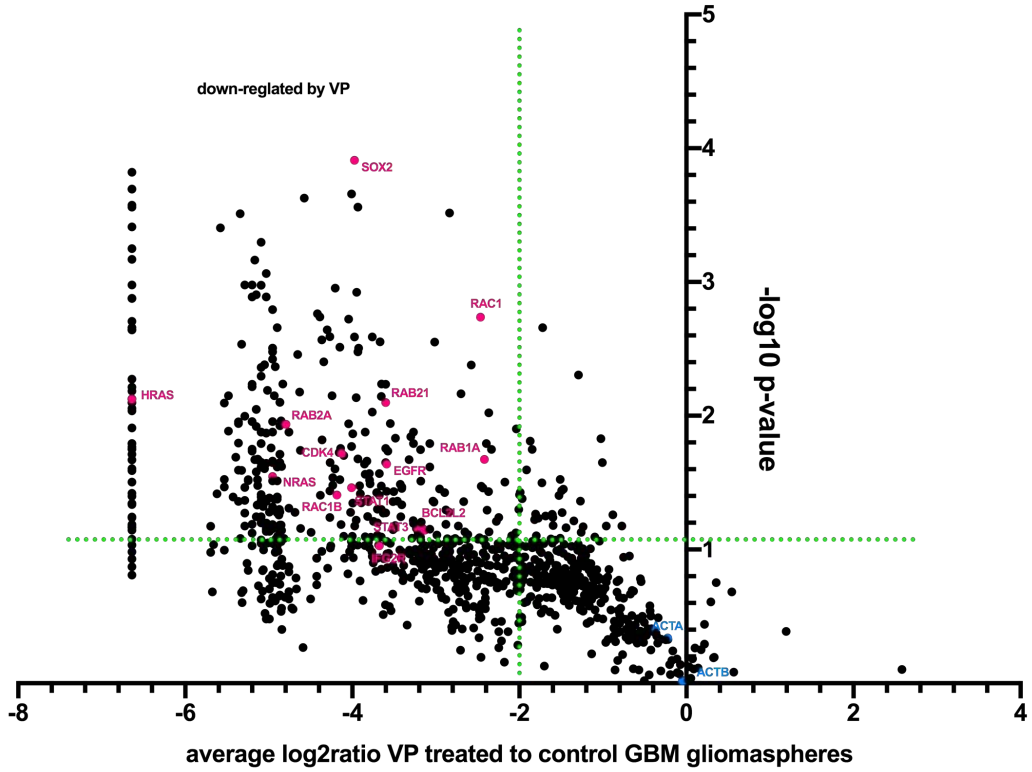

Figure S10: Short-term treatment of GSCs with Verteporfin reduces protein expression

GBM301 and pGBM2 (both $EGFR^{vIII}$) and GBM1219 (EGFR wild-type) GSCs were treated with VP for 6 hours and subjected to label-free total proteomic profiling. Volcano plot showing individual proteins graphed by log2 ratio and -log10 of p-value from t-tests comparing protein levels in all VP treated GSC lines to control GSC lines. The vertical green dashed line demarcates proteins that show ≥2-fold of decrease in expression induced by VP treatment and the horizontal green line demarcates p-values ≥.05. Pink highlights proteins that show reduced protein levels in response to VP that have been confirmed by immunoblot (see Figure S11). Blue shows ACTIN control proteins, which did not change in response to VP treatment.

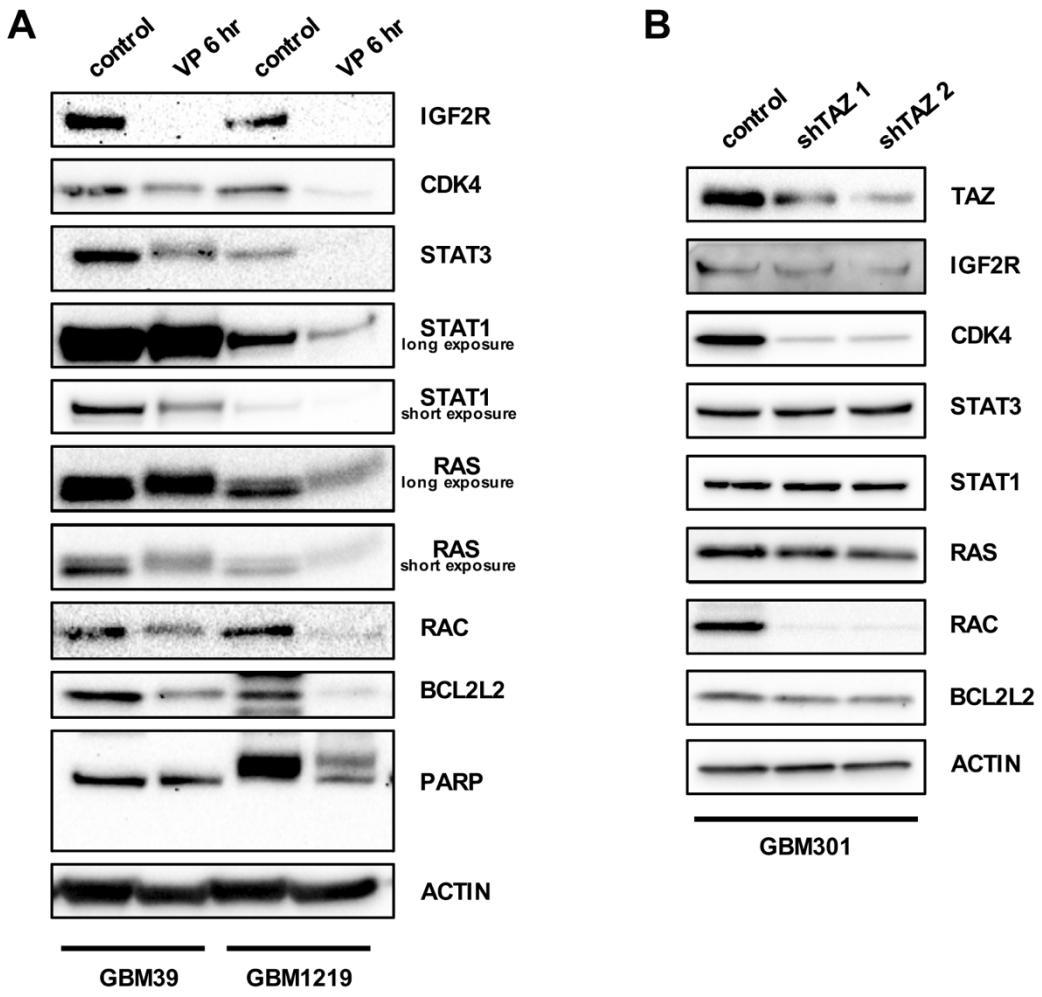

Figure S11: Short-term pre-treatment of GSCs with Verteporfin reduces expression of YAP/TAZ-dependent and independent target genes

(A) GBM39 and GBM1219 GSCs treated with VP for 6 hours, at which times apoptosis was not readily detected, as indicated by immunoblotting for PARP cleavage. Confirmatory immunoblots for several proteins that showed significantly reduced expression by proteomic profiling, including proteins that control cell proliferation (CDK4), signaling (IGF2R, STAT3, STAT1, RAS proteins, RAC proteins) and cell survival (BCL2L2).
(B) Lentiviral shRNA knockdown of TAZ in GBM301 GSCs caused decreased protein expression of several proteins that are targeted by VP treatment (IFG2R, CDK4, RAC proteins), but not of others (STAT3, STAT1, RAS, BCL2L2). Cells were treated with ZVAD (20 μM) to prevent apoptosis and preserve signaling pathways and harvested 3 days post-infection.

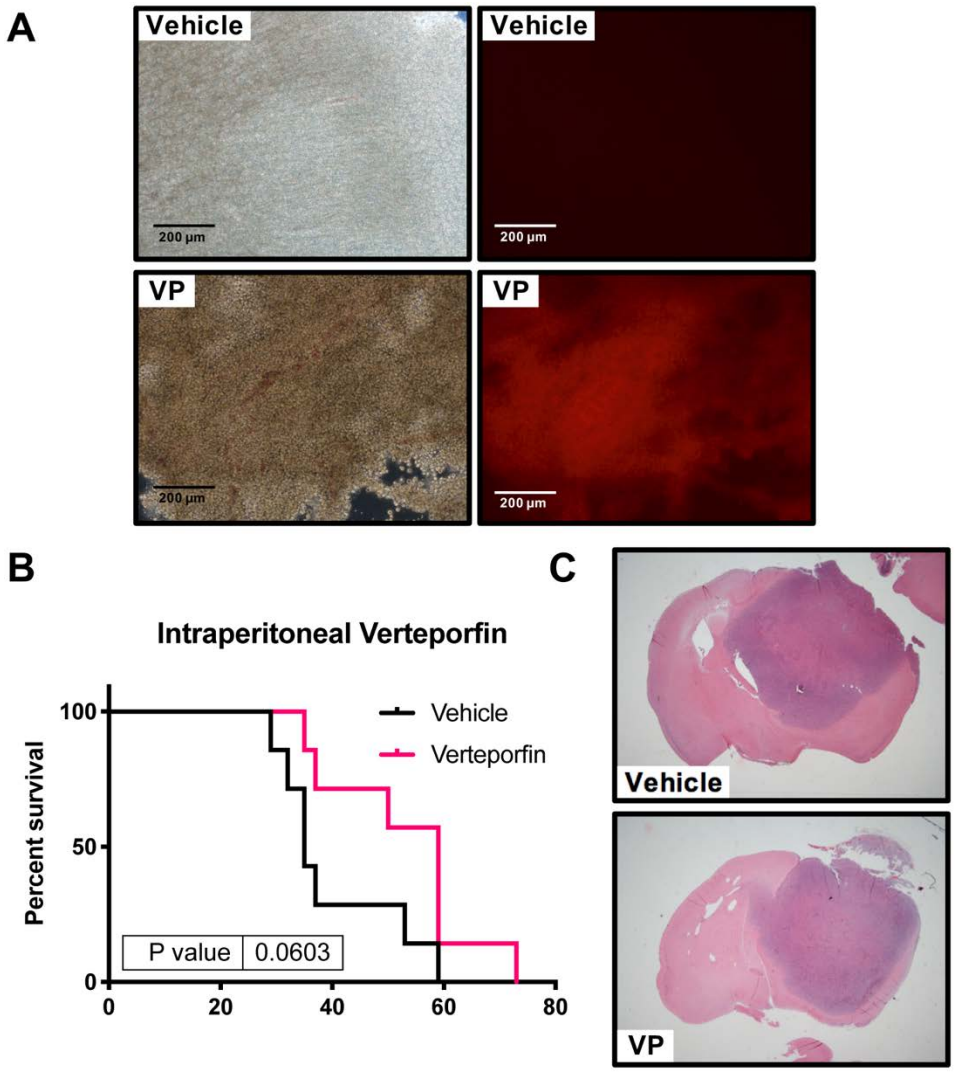

Figure S12: Intraperitoneal delivery of Verteporfin was detected in tumor-bearing mice and extended survival

(A) Representative micrographs of unfixed brain tissue sections from GBM39 xenografts in NSG mice showing VP absorption into brain tumor tissue following IP injection. Xenograft-bearing NSG mice were injected IP with Visudyne (pharmaceutical grade liposomal VP) at 100 mg/kg or with saline (vehicle), their brains removed 6-8 hours following injection to allow for VP to enter the circulatory system and brain, and their unfixed brains sliced into sections with a vibratome. VP absorption was visualized by fluorescence microscopy for far red emission in response to blue light excitement (390-435 nm/620-680 nm band pass filter set).
(B) Kaplan-Meir survival curve from orthotopic tumor-bearing mice that indicates a survival benefit for VP-treated mice. Mice were treated with Visudyne by IP injection at 100 mg/kg every other day for a total of 8 doses over two weeks; control animals were treated by IP injection of equivalent volumes of sterile phosphate-buffered saline for a total of 8 times for two weeks. No gross toxicities were observed from Visudyne treatment. Statistical test for survival curve performed with Log-rank (Mantel-Cox) test, (n=7 for each treatment group).
(C) Representative images from H&E stained brain sections from mice at the survival endpoints from vehicle and VP-treated experimental arms.

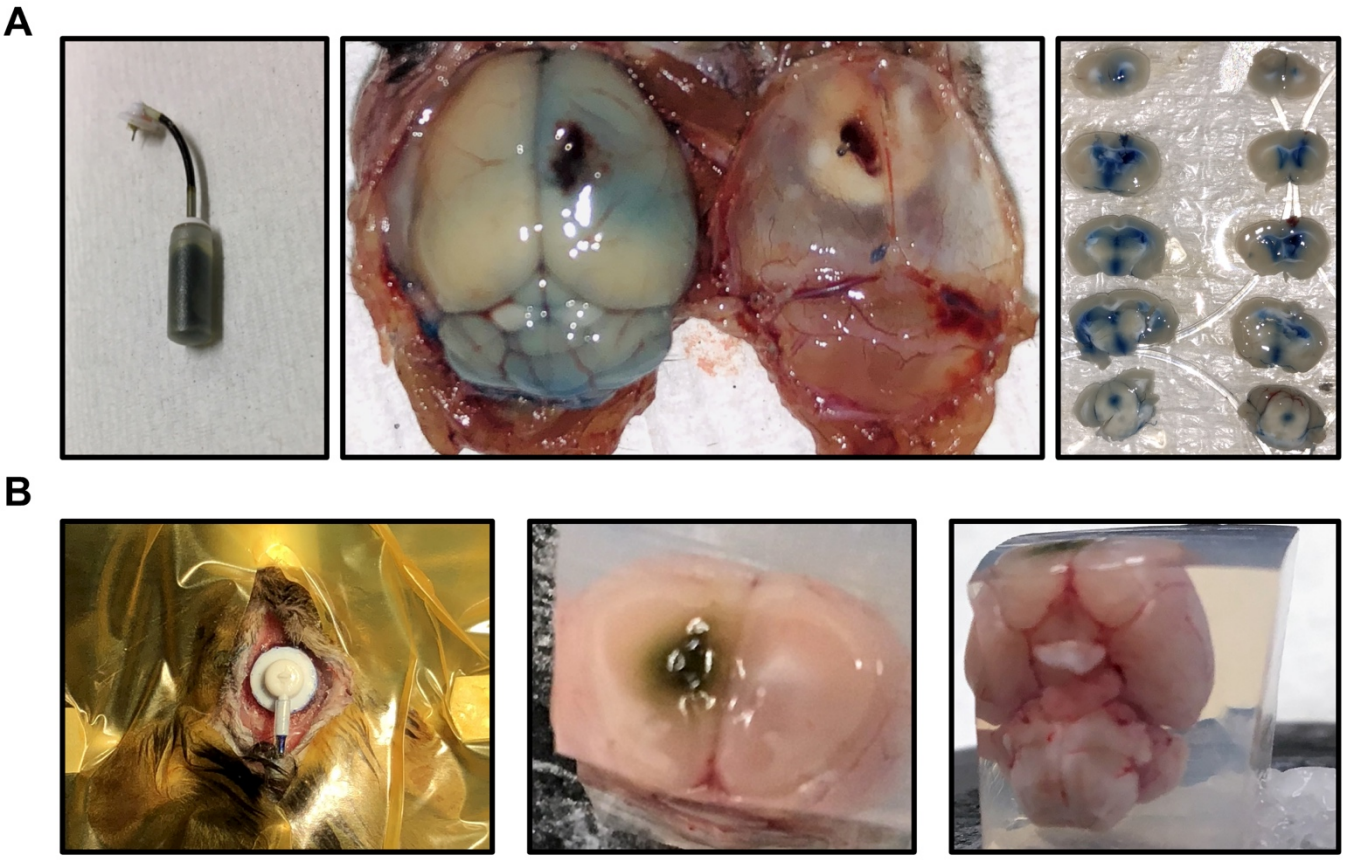

Figure S13: Osmotic pump implantation and proof of concept

(A) Images depicting Alzet micro-osmotic pump assembly (left) and successful delivery of evans blue dye on a trial run of pump implantation (middle and right). Osmotic pumps were assembled, filled with dye, and primed in saline at 37°C overnight before implantation. Mice were implanted with pump cannula 1 mm laterally to the right and 0.5 mm posterior to bregma and sacrificed 72 hours after pump implantation to visualize dye localization and pump placement efficiency.
(B) Images depicting pump cannula placement onto mouse skull for VP-filled pump (left), and visualization of VP absorption (VP is visibly dark green) upon removal of mouse brain and preparation for sectioning, which was used in **Figure 6A**. Osmotic pump was loaded as in panel (**A)** with liposomal VP (200 mg in 100 ml, Visudyne) and implanted into mice for fourteen days of continuous drug delivery. Unfixed brains from mice were then immobilized into agarose blocks for vibratome sectioning (right).

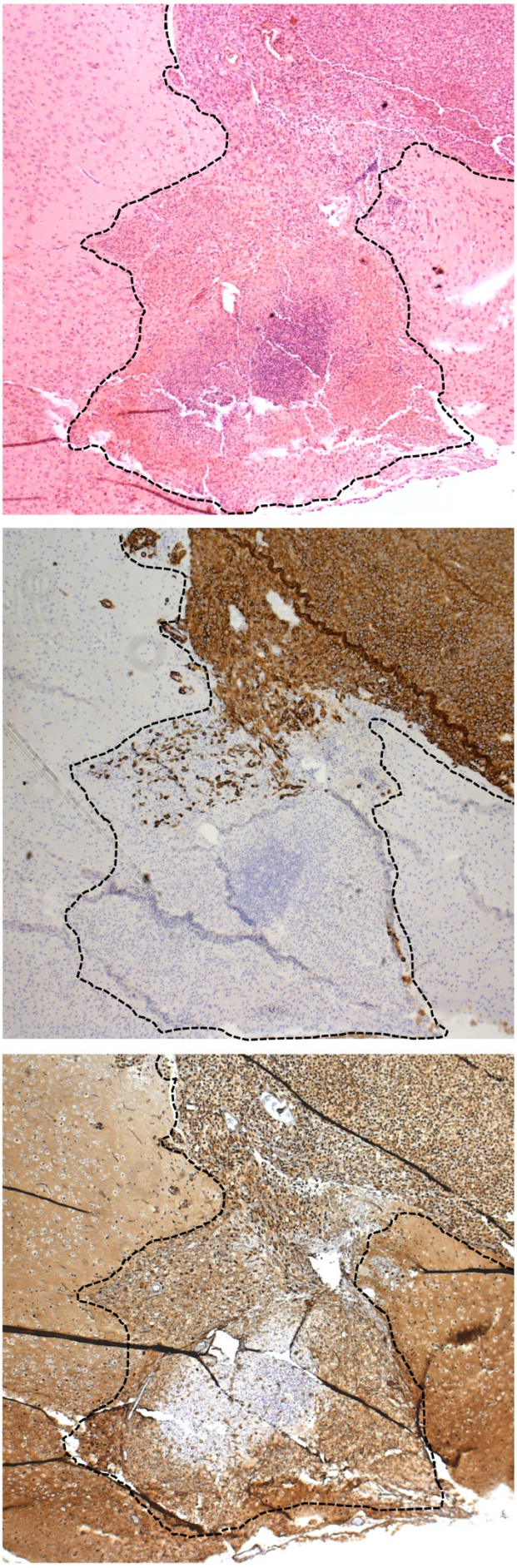

Figure S14: Verteporfin treatment results in tumor necrosis and decreased expression of EGFR and SOX2

Low magnification images of a representative GBM xenograft tumor mass after treatment with VP by osmotic pump. Images of H&E (top), and IHC staining for EGFR (middle) and SOX2 (bottom) expression are matched to the tumor location imaged in Figure 5 in the region treated with VP by osmotic pump. Dashed outline shows full extent of tumor growth and infiltration. H&E used to score for necrosis and tissue viability and to evaluate tumor size and location.

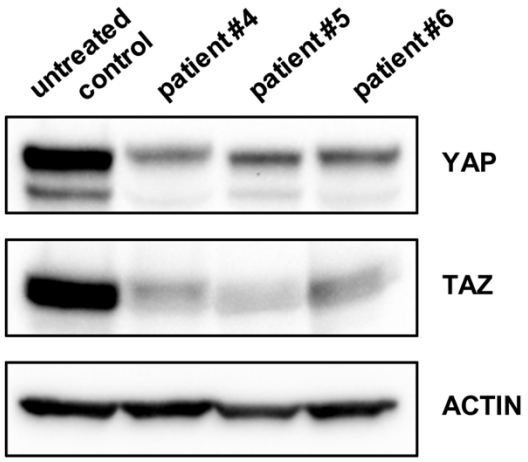

(Visudyne) treated patients

Total tissue lysates from GBM surgical specimens blotted for YAP and TAZ total protein. Tumor tissue from all patients was collected under similar conditions intraoperatively, flash frozen on dry ice, and lyzed directly in RIPA buffer upon thawing before immunoblotted. For liposomal VP (Visudyne) treated patients (patients #4, 5, 6 on Table S5), intraoperative fluorescence was used during surgery to illuminate the tumor bed during resection, such that light exposure may have affected the tumor tissue. The untreated control case chosen for comparison is tumor tissue from a representative EGFR-amplified case, from a patient that did not receive VP or intraoperative fluorescence. Note that we cannot be certain that these tumors all expressed equivalent levels of YAP and TAZ prior to Verteporfin infusion or intraoperative fluorescence or tissue collection, so we can cannot necessarily attribute differences in YAP and TAZ protein expression levels between patients to Visudyne treatment.

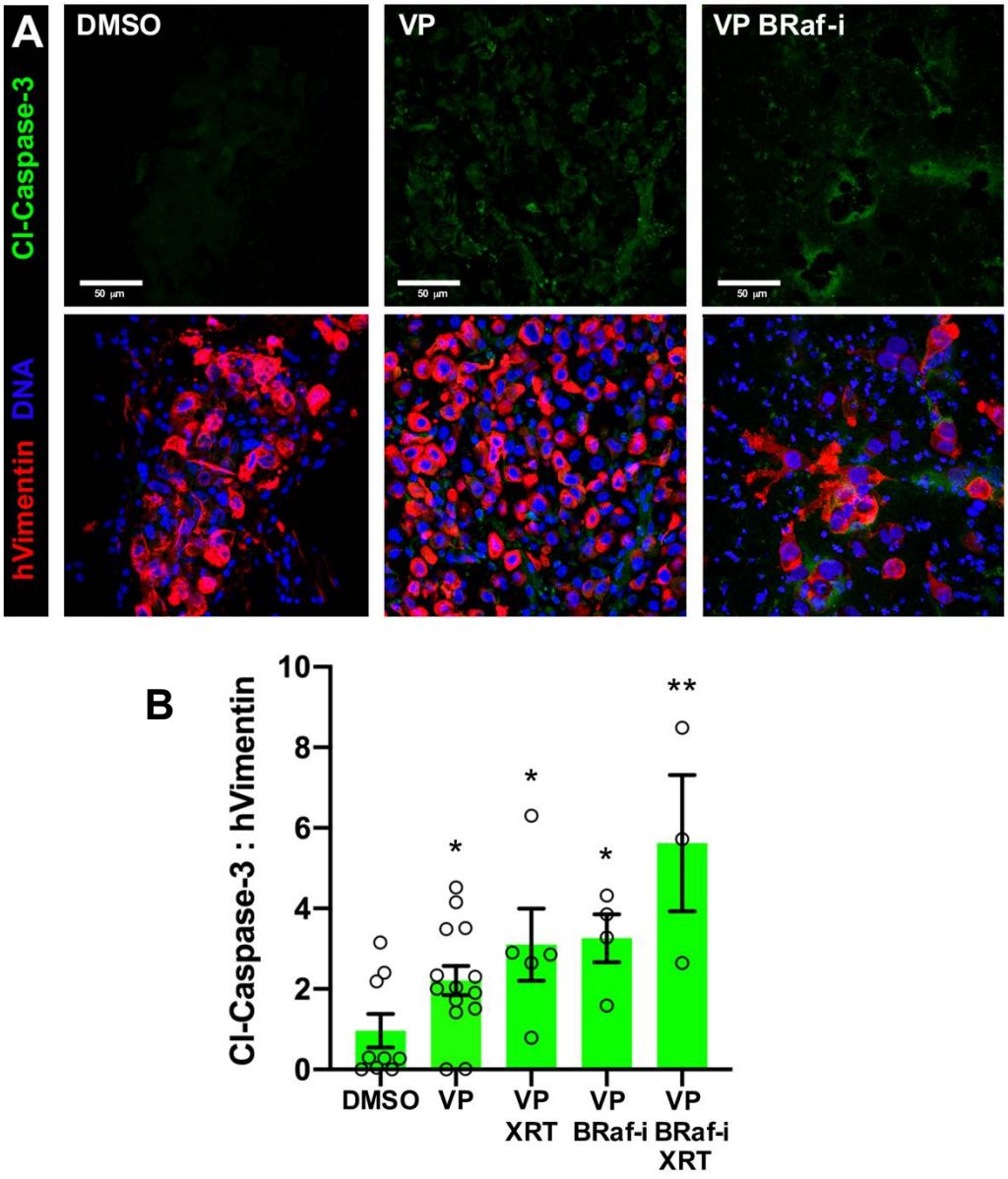

Figure S16: Apoptosis in response to Verteporfin is enhanced by combination therapy

Ex vivo organotypic slice cultures created from GBM39 xenografts implanted into NSG mice, treated with DMSO (control), 1 μg/mL VP for 24 hours, and/or other indicated agents, and then stained and imaged with confocal microscopy. DRAQ7 DNA dye (blue) labels all cell nuclei in tumor and stroma. VP was combined with concurrent 10 μM dabrafenib (BRaf-inhibitor, 24 hrs) and/or 2 Gy of radiation (XRT) delivered 12 hrs following VP addition.
(A) Immunostaining for cleaved-Caspase-3 (Cl-Caspase-3, green, upper panels), labeling apoptotic cells, and human Vimentin (hVimentin, red, lower panels overlay), which specifically labels human tumor cells in the mouse brain parenchyma.
(B) Ratios for total cleaved-Caspase-3 and hVimentin immunostaining in organotypic slice cultures; values measured in 30-50 μm confocal z-stacks using Imaris.
* p<.05; ** p<.01 with ANOVA multiple comparisons test.

stock ID number	CG number	gene name	*dEGFR$^{\lambda}$;dp110^{CAAX} phenotype*	wild-type phenotype
b27661	CG11228	hippo	E	no obvious effect
v104169	CG11228	hippo	E	no obvious effect
v106174	CG12072	warts	E	no obvious effect
v9928	CG12072	warts	E	no obvious effect
b34067	CG4005	yorkie	SS	no obvious effect
v109756	CG4005	yorkie	SS	no obvious effect
b55404	CG3595	scalloped	SS	
b35481	CG3595	scalloped	SS	
v60101		40D-UAS control	no effect	no effect

Table S1. Testing dsRNAs targeting Hippo-Yki pathway.
VDRC stock ID numbers prefaced by "v," Bloomington stock ID numbers prefaced by "b." Bold highlights stocks that yielded reproducible genetic interactions and clear phenotypic alterations. Key to genetic interactions: E: enhancer SS: strong suppressor, WS: weak suppressor; no effect indicates that there were no obvious phenotypic differences between the dsRNA and control animals; nd indicates not determined. All UAS-dsRNAs expressed from in glia by the repo-Gal4 driver.

	Sex	*Age*	*Dose*	*Drug-Related Side Effects*	*Intra-op Flour*	*Pathology*	*Follow-up*
Patient 1	M	51	0.15mg/kg	None	None	Necrosis	Died 1/1/19 14 months
Patient 2	F	62	0.3mg/kg	None	Yes	Therapy-related changes with residual / recurrent GBM	3/3/19 13 months
Patient 3	M	62	0.3mg/kg	None	Yes	GBM	6/14/19 13 months
Patient 4	M	60	0.3mg/kg	None	Yes	GBM	12/11/18 Lost to follow up 4 months
Patient 5	M	33	0.3mg/kg	None	Yes	GBM, IDH Mut	12/7/18 Lost to follow up 4 months
Patient 6	M	38	0.3mg/kg	None	Yes	GBM	6/20/19

Table S2. Patient information for phase 0 clinical trial.
Six patients were administered Visudyne prior to surgical resection or recurrent disease. Patient sex and age are listed along with dose of medication administered. Dose was escalated to 0.3mg/kg after the first patient tolerated infusion and there was no evidence of fluorescence, however, this may have been a consequence of the lesion being consistent with radiation necrosis rather than recurrent glioblastoma. There were no drug related side effects. The end goal of this study was to identify qualitative intra-operative fluorescence (Yes/No) and collect tissue for post-operative qualitative and quantitative analysis. We were able to successfully demonstrate drug uptake in patients with glioblastoma.

Table S3. List of Abbreviations, Acronyms, and Symbols.

5-ALA: 5-aminolevulinic acid, protoporphyrin IX precursor
bp: base pair
CNS: central nervous system
CAAX: CAAX prenylation sequence
ChIP: chromatin-immunoprecipitation
CDK1: cyclin-dependent kinase 1, gene and protein name
C-MYC: transcription factor, gene and protein name
DMSO: dimethyl sulfoxide
Drosophila: Drosophila melanogaster, vinegar or fruit fly
EGFR: Epidermal Growth Factor Receptor, gene and protein name
$EGFR^{vIII}$: Epidermal Growth Factor Receptor, mutant variant III
FDA: Food and Drug Administration
GBM, GBMs: glioblastoma
GFP: green-fluorescent protein, gene and protein name
GSC: gliomasphere, serum-free neurosphere culture of glioblastoma tumor stem-like cells
hNPC, hNPCs: human neural progenitor cells
IGF2: Insulin-like Growth Factor 2, gene and protein name
IHC: immunohistochemistry
IND: investigational new drug application
Ink4a/Arf-/- : mouse gene name, products of the CDKN2A locus, tumor suppressors, gene and protein names
IP: intraperitoneal injection
IV: intravenous injection
LATS1: Large Tumor Suppressor Kinase 1, gene and protein name
LATS2: Large Tumor Suppressor Kinase 2, gene and protein name
MET: MET receptor tyrosine kinase, gene and protein name
mNSC, mNSCs: mouse neural stem cells
mRNA: messenger RNA
MST1: Hippo kinase 1, gene and protein name
MST2: Hippo kinase 2, gene and protein name
PDGFRA: PDGFalpha receptor, gene and protein name
PI3K: Phopho-inositol-3 kinase, Pi-3 kinase, a cell signaling pathway
PPIX: protoporphyrin IX, porphyrin
PTEN: Phosphatase and tensin homolog, lipid phosphatase for Phopho-inositol-3
qPCR: quantitative PCR
RAF: protein kinase, named for virus-induced Rapidly Accelerated Fibrosarcoma, gene and protein name
Ras: small GTPase that acts downstream of RTKs and upstream of RAF
RNAseq: mRNA isolation coupled with next generation sequencing
RTK: Receptor-tyrosine kinase, a cell signaling pathway linked to Ras and RAF
RNAi: RNA-interference method of gene silencing
Sd: Scalloped transcription factor, Drosophila melanogaster, gene and protein name
shRNAs: small-hairpin RNAs, used for RNAi
SOX2: SRY-box 2 transcription factor, gene and protein name
TAZ: transcriptional coactivator with PDZ-binding motif, gene and protein name
TCGA: The Cancer Genome Atlas
TEAD: TEA domain proteins, gene and protein name
TMA: tissue microarray
VP: Verteporfin
XRT: ionizing radiation
Yki: Yorkie transcription factor, Drosophila melanogaster, gene and protein name
YAP: Yes-associated Protein 1, YAP1 transcription factor, gene and protein name
ZVAD: Z-VAD-FMK, carbobenzoxy-valyl-alanyl-aspartyl-[O-methyl]-fluoromethylketone, pan-caspase inhibitor

Sample	Genotype		Genotype	IHC results		
Tumor	EGFR status	Other RTKs	other genetic lesions, genomics results	EGFR	TAZ	YAP
131			PTEN loss, NTRK2 overexpression	4	3	3
923		PDGFRA amp	SOX2 amp; AKT gain; CDKN2A loss	4	2	4
128B	EGFR gain		MDM4 PIK3C2B gain; PTEN CdkN2a loss	4	3	4
29	EGFR amp		PI3KC2B, MDM4 gain; PTEN LOH	4	4	4
430	EGFR amp		CDKN2A and PTEN loss	4	3	4
211	EGFR amp		PTEN TP53 loss	3	3	3
724			IDH1 mutant; CIC TP53 loss	2	1	1
222			CDK4, CDK6 amp; SOX2 gain; PTEN loss	3	3	4
729	EGFR gain	NTRK3 amp	NMYC gain; PTEN, ATRX loss	3	2	3
925	EGFR amp		MDM2 gain; PTEN CDKN2A loss; MGMT methylation	4	3	3
508		PDGFRA amp	PIK3C2B mutation	2	1	1
914	EGFR amp		PTEN, TP53 loss; GLI3 amp	4	1	4
1215		PDGFRA, KIT gain	PTEN CDKN2A loss; MGMT methylation	1	2	2
212A	EGFR gain	MET amp	PIK3CA gain; PTEN LOH; TP53 NF1, and CDKN2A loss	3	3	3
1023B			IDH mutant; MGMT methylation	2	1	2
1023A		PDGFRA amp	BRAF MDM2 amp	1	0	2
1219	EGFR amp		PTEN loss, SHH gain	4	3	4
109A		PDGFRA, KIT gain	SOX2 amp; RB1 CDKN2A loss; PTEN LOH	2	3	4
1217			TP53, PTEN, CDKN2A loss	2	1	2
915	EGFR amp		PTEN, CDKN2A loss	4	3	4
911	EGFR gain	MET gain	NOTCH1 gain, CDKN2A loss	4	3	3
109B	EGFR gain		NF1, CDKN2A, PTEN loss	3	3	3
212B	EGFR gain		PTEN LOH; CDKN2A and RB1 loss	3	4	3
114		IDH1	IDH1 mutant; CMYC, WNT5A, YES1 amp	1	0	1
79	EGFR gain		CDKN2A loss	3	3	4
417	EGFR gain	MET gain	TP53, NF1, RB1 loss	3	1	3
1118		MET amp	whole chromosome 10 LOH	nd	3	4
126	EGFR amp		PTEN, CDKN2A loss, QKI loss	4	3	4

Table S4: Tally of tumor mutations and phenotypes in TMA GBM specimens.
Each diagnosis of glioblastoma multiforme grade IV was reconfirmed by histopathology. Tissues selected for the TMA were reviewed by a neuropathologist for tumor phenotype and cellularity. 2-4 tissue specimens from 1-2 paraffin blocks for each tumor were selected and core regions were used to create the TMA. Curated tumor genotype from FISH, Oncoscan copy number arrays, and/or RNAseq genomic profiling for all tumor specimens used for IHC data for YAP, TAZ, and EGFR expression. IHC data was scored on a 1-4 scale for signal intensity specific to tumor cells, and, for YAP and TAZ, nuclear localization.

Table S5

Gene Description	Gene	log2ratio VP treated/control	p-value
Malectin	MLEC	-6.64	0.0022
Transducin beta-like protein 2	TBL2	-6.64	0.0249
Isoform 4 of Rabankyrin-5	ANKFY1	-6.64	0.0088
Isoform 2 of Galactokinase	GALK1	-6.64	0.0013
Putative peptidyl-tRNA hydrolase PTRHD1	PTRHD1	-6.64	0.0013
Isoform B of Nucleoporin SEH1	SEH1L	-6.64	0.0171
Deoxyribose-phosphate aldolase	DERA	-6.64	0.0006
CDGSH iron-sulfur domain-containing protein 1	CISD1	-6.64	0.0092
Isocitrate dehydrogenase [NAD] subunit gamma, mitochondrial	IDH3G	-6.64	0.0380
CD97 antigen	CD97	-6.64	0.0053
Exocyst complex component 1	EXOC1	-6.64	0.0075
Peflin	PEF1	-6.64	0.0002
Isoform 2 of Peroxisomal acyl-coenzyme A oxidase 1	ACOX1	-6.64	0.0023
A-kinase anchor protein 8	AKAP8	-6.64	0.0013
Metaxin-2	MTX2	-6.64	0.0023
DNA primase small subunit	PRIM1	-6.64	0.0214
Fatty acid desaturase 2	FADS2	-6.64	0.0178
Rab3 GTPase-activating protein catalytic subunit	RAB3GAP1	-6.64	0.0011
Zinc finger CCCH-type antiviral protein 1-like	ZC3HAV1L	-6.64	0.0002
Peptidyl-tRNA hydrolase 2, mitochondrial	PTRH2	-6.64	0.0003
Phosphoglycolate phosphatase	PGP	-6.64	0.0161
Exocyst complex component 7	EXOC7	-6.64	0.0178
Peroxisomal acyl-coenzyme A oxidase 1	ACOX1	-6.64	0.0065
Isoform 2 of Rab3 GTPase-activating protein catalytic subunit	RAB3GAP1	-6.64	0.0020
NHL repeat-containing protein 2	NHLRC2	-6.64	0.0075
Protein sel-1 homolog 1	SEL1L	-6.64	0.0004
ATP-dependent Clp protease proteolytic subunit, mitochondrial	CLPP	-6.64	0.0453
Polypeptide N-acetylgalactosaminyltransferase 2	GALNT2	-6.64	0.0460
Isoform 2 of Fatty aldehyde dehydrogenase	ALDH3A2	-6.64	0.0161
Golgi resident protein GCP60	ACBD3	-6.64	0.0061
Nucleoporin Nup43	NUP43	-6.64	0.0080
Mitochondrial carrier homolog 2	MTCH2	-6.64	0.0007
Isoform 3 of Signal peptidase complex catalytic subunit SEC11A	SEC11A	-6.64	0.0075
Phosphatidylinositide phosphatase SAC1	SACM1L	-6.64	0.0123
GTPase HRas	HRAS	-6.64	0.0075
39S ribosomal protein L17, mitochondrial	MRPL17	-6.64	0.0023
Ragulator complex protein LAMTOR3	LAMTOR3	-6.64	0.0003
Protein O-GlcNAcase	MGEA5	-6.64	0.0013
SPARC	SPARC	-6.64	0.0257

Gene Description	Gene	log2ratio VP treated/control	p-value
E3 ubiquitin-protein ligase RING1	RING1	-6.64	0.0013
Integrin-linked protein kinase	ILK	-6.64	0.0013
Poly(ADP-ribose) glycohydrolase ARH3	ADPRHL2	-6.64	0.0194
Short coiled-coil protein	SCOC	-6.64	0.0080
Syntaxin-binding protein 3	STXBP3	-6.64	0.0075
Selenocysteine-specific elongation factor	EEFSEC	-6.64	0.0002
Isoform 4 of E3 ubiquitin-protein ligase TRIM9	TRIM9	-6.64	0.0023
Transmembrane protein 41B	TMEM41B	-6.64	0.0399
3-ketoacyl-CoA thiolase, peroxisomal	ACAA1	-6.64	0.0453
Isoform 5 of Oxysterol-binding protein-related protein 6	OSBPL6	-6.64	0.0314
Isoform 2 of Calnexin	CANX	-5.62	0.0384
Cytochrome c oxidase subunit 2	MT	-5.58	0.0004
Isocitrate dehydrogenase [NAD] subunit, mitochondrial	IDH3B	-5.53	0.0341
Sideroflexin-3	SFXN3	-5.53	0.0299
Dynein light chain 2, cytoplasmic	DYNLL2	-5.53	0.0080
Isoform 5 of AP-3 complex subunit delta-1	AP3D1	-5.48	0.0130
Cleavage and polyadenylation specificity factor subunit 3	CPSF3	-5.48	0.0071
Guanine nucleotide-binding protein subunit alpha-11	GNA11	-5.43	0.0405
Echinoderm microtubule-associated protein-like 4	EML4	-5.40	0.0205
ADP-ribosylation factor-like protein 8A	ARL8A	-5.36	0.0111
39S ribosomal protein L39, mitochondrial	MRPL39	-5.36	0.0255
Ribose-5-phosphate isomerase	RPIA	-5.36	0.0437
UPF0488 protein C8orf33	C8orf33	-5.36	0.0114
7SK snRNA methylphosphate capping enzyme	MEPCE	-5.36	0.0160
Mitochondrial import receptor subunit TOM70	TOMM70A	-5.34	0.0003
Isoform 2 of Caseinolytic peptidase B protein homolog	CLPB	-5.33	0.0257
E3 ubiquitin-protein ligase CHIP	STUB1	-5.33	0.0029
E3 UFM1-protein ligase 1	UFL1	-5.29	0.0428
DDB1- and CUL4-associated factor 7	DCAF7	-5.29	0.0101
Protein FAM3C	FAM3C	-5.29	0.0011
Cyclin-dependent kinase 2	CDK2	-5.29	0.0344
Nucleobindin 2, isoform CRA_b	NUCB2	-5.25	0.0305
RNA-binding protein Musashi homolog 1	MSI1	-5.25	0.0300
Cytochrome c oxidase subunit 4 isoform 1, mitochondrial	COX4I1	-5.20	0.0011
39S ribosomal protein L3, mitochondrial	MRPL3	-5.20	0.0058
Hepatitis B virus x interacting protein	LAMTOR5	-5.20	0.0061
Apolipoprotein O	APOO	-5.20	0.0111
Ragulator complex protein LAMTOR5	LAMTOR5	-5.20	0.0061
Protein canopy homolog 3	CNPY3	-5.20	0.0111
NADPH--cytochrome P450 reductase	POR	-5.20	0.0184

Gene Description	Gene	log2ratio VP treated/control	p-value
Serine/threonine-protein kinase PRP4 homolog	PRPF4B	-5.20	0.0178
AH receptor-interacting protein	AIP	-5.20	0.0013
Succinyl-CoA ligase [ADP/GDP-forming] subunit alpha, mitochondrial	SUCLG1	-5.17	0.0007
Replication protein A 14 kDa subunit	RPA3	-5.17	0.0213
Beta-catenin-like protein 1	CTNNBL1	-5.15	0.0012
26S proteasome non-ATPase regulatory subunit 7	PSMD7	-5.15	0.0262
Glutamate-rich WD repeat-containing protein 1	GRWD1	-5.15	0.0090
Peptidyl-prolyl cis-trans isomerase H	PPIH	-5.15	0.0120
Isoform 2 of Mannose-1-phosphate guanyltransferase beta	GMPPB	-5.15	0.0090
Protein LYRIC	MTDH	-5.14	0.0466
Nuclear pore complex protein Nup133	NUP133	-5.14	0.0466
Catenin delta-1	CTNND1	-5.14	0.0300
Protein lunapark	LNP	-5.13	0.0211
Nuclear pore complex protein Nup160	NUP160	-5.13	0.0332
Carnitine O-palmitoyltransferase 2, mitochondrial	CPT2	-5.12	0.0215
Isoform 4 of Protein lunapark	LNP	-5.09	0.0387
Pachytene checkpoint protein 2 homolog	TRIP13	-5.09	0.0241
Protein LSM14 homolog A	LSM14A	-5.09	0.0223
Isoform 2 of Peptidyl-prolyl cis-trans isomerase FKBP8	FKBP8	-5.09	0.0011
Polycomb protein SUZ12	SUZ12	-5.09	0.0011
39S ribosomal protein L47, mitochondrial	MRPL47	-5.09	0.0044
Mitochondrial fission 1 protein	FIS1	-5.09	0.0132
Acyl-protein thioesterase 2	LYPLA2	-5.09	0.0005
ADP-ribosylation factor-like protein 8B	ARL8B	-5.09	0.0051
Succinate dehydrogenase [ubiquinone] iron-sulfur subunit, mitochondrial	SDHB	-5.09	0.0433
ATP-dependent Clp protease ATP-binding subunit clpX-like, mitochondrial	CLPX	-5.09	0.0161
pre-rRNA processing protein FTSJ3	FTSJ3	-5.09	0.0132
Putative GTP cyclohydrolase 1 type 2 NIF3L1	NIF3L1	-5.09	0.0405
Glutathione peroxidase (Fragment)	GPX4	-5.09	0.0243
Glutathione peroxidase (Fragment)	GPX4	-5.09	0.0223
Isoform 5 of Ubiquitin carboxyl-terminal hydrolase 19	USP19	-5.09	0.0161
TIP41-like protein	TIPRL	-5.07	0.0478
Sideroflexin-1	SFXN1	-5.05	0.0042
Eukaryotic translation elongation factor 1 epsilon-1	EEF1E1	-5.05	0.0249
Reticulon-1	RTN1	-5.05	0.0420
Mitochondrial Rho GTPase 2	RHOT2	-5.03	0.0135
Intron-binding protein aquarius	AQR	-5.03	0.0013
EH domain-containing protein 1	EHD1	-5.03	0.0135
28S ribosomal protein S23, mitochondrial	MRPS23	-5.03	0.0437
EH domain-containing protein 1	EHD1	-5.03	0.0135

Gene Description	Gene	log2ratio VP treated/control	p-value
Isoform 2 of 3'(2'),5'-bisphosphate nucleotidase 1	BPNT1	-5.03	0.0226
Mitochondrial import inner membrane translocase subunit Tim9	TIMM9	-5.03	0.0009
Isoform 3 of Fermitin family homolog 2	FERMT2	-5.02	0.0065
3-hydroxyisobutyryl-CoA hydrolase, mitochondrial	HIBCH	-4.99	0.0412
Isoform 4 of Pyruvate dehydrogenase E1 component subunit alpha, somati	PDHA1	-4.97	0.0174
Vacuolar protein sorting-associated protein 29	VPS29	-4.95	0.0016
Guanine nucleotide-binding protein G(q) subunit alpha	GNAQ	-4.95	0.0033
Tricarboxylate transport protein, mitochondrial	SLC25A1	-4.95	0.0224
Pleiotropic regulator 1	PLRG1	-4.95	0.0031
GTPase NRas	NRAS	-4.95	0.0285
Cation-dependent mannose-6-phosphate receptor	M6PR	-4.95	0.0224
Aldehyde dehydrogenase family 16 member A1	ALDH16A1	-4.95	0.0481
NAD kinase 2, mitochondrial	NADK2	-4.95	0.0031
3'(2'),5'-bisphosphate nucleotidase 1	BPNT1	-4.95	0.0307
E3 ubiquitin-protein ligase BRE1A	RNF20	-4.95	0.0218
Isoform 3 of Peptidyl-prolyl cis-trans isomerase E	PPIE	-4.95	0.0033
Pyruvate dehydrogenase protein X component, mitochondrial	PDHX	-4.95	0.0111
Protein ABHD14A-ACY1	ABHD14A	-4.95	0.0031
Syndecan binding protein (Syntenin), isoform CRA_a	SDCBP	-4.95	0.0038
UPF0587 protein C1orf123	C1orf123	-4.95	0.0132
OS=Homo sapiens GN=NUCB1 PE=1 SV=4	NUCB1	-4.93	0.0071
Endoplasmic reticulum resident protein 44	ERP44	-4.93	0.0420
NADH dehydrogenase [ubiquinone] flavoprotein 1, mitochondrial	NDUFV1	-4.92	0.0043
Protein BUD31 homolog	BUD31	-4.90	0.0022
Lamin-B receptor	LBR	-4.90	0.0420
NADH dehydrogenase [ubiquinone] 1 alpha subcomplex subunit 10, mitoch	NDUFA10	-4.90	0.0405
Importin subunit alpha-4	KPNA3	-4.90	0.0241
cAMP-dependent protein kinase catalytic subunit alpha	PRKACA	-4.90	0.0307
Ras GTPase-activating-like protein IQGAP2	IQGAP2	-4.90	0.0405
Isoform Mitochondrial of Lysine--tRNA ligase	KARS	-4.87	0.0502
Isoform 2 of 5'-nucleotidase domain-containing protein 2	NT5DC2	-4.87	0.0119
Golgi phosphoprotein 3	GOLPH3	-4.87	0.0079
Basigin	BSG	-4.87	0.0194
Inositol-3-phosphate synthase 1	ISYNA1	-4.87	0.0224
Pre-mRNA-processing factor 6	PRPF6	-4.87	0.0079
Alpha-globin transcription factor CP2	TFCP2	-4.87	0.0194
Enhancer of mRNA-decapping protein 3	EDC3	-4.87	0.0194
Very-long-chain 3-oxoacyl-CoA reductase	HSD17B12	-4.85	0.0109
Isoform 3 of Malignant T-cell-amplified sequence 1	MCTS1	-4.85	0.0239
Huntingtin-interacting protein K	HYPK	-4.83	0.0058

Gene Description	Gene	log2ratio VP treated/control	p-value
60S ribosomal protein L36a-like	RPL36AL	-3.95	0.0012
2',3'-cyclic-nucleotide 3'-phosphodiesterase	CNP	-3.93	0.0211
Syntaxin-12	STX12	-3.93	0.0033
Peripheral plasma membrane protein CASK	CASK	-3.93	0.0003
Dynamin-1	DNM1	-3.92	0.0031
Succinate dehydrogenase [ubiquinone] flavoprotein subunit, mitochondrial	SDHA	-3.91	0.0334
Nuclear pore complex protein Nup153	NUP153	-3.90	0.0383
Isoform 3 of Nuclear pore complex protein Nup153	NUP153	-3.90	0.0383
Vacuolar protein sorting-associated protein 4B	VPS4B	-3.89	0.0448
3-ketoacyl-CoA thiolase, mitochondrial	ACAA2	-3.85	0.0229
Serine/threonine-protein phosphatase PGAM5, mitochondrial	PGAM5	-3.85	0.0132
Pyrroline-5-carboxylate reductase 2	PYCR2	-3.85	0.0274
Eukaryotic translation initiation factor 2A	EIF2A	-3.83	0.0218
NADH dehydrogenase [ubiquinone] 1 alpha subcomplex subunit 8	NDUFA8	-3.82	0.0420
Septin 10, isoform CRA_c	SEPT10	-3.81	0.0439
Adenylate kinase 4, mitochondrial	AK4	-3.80	0.0270
Apoptosis-inducing factor 1, mitochondrial	AIFM1	-3.79	0.0303
Actin-related protein 2/3 complex subunit 1A	ARPC1A	-3.79	0.0323
Lysosome-associated membrane glycoprotein 1	LAMP1	-3.76	0.0094
NADPH:adrenodoxin oxidoreductase, mitochondrial	FDXR	-3.76	0.0026
Isoform 3 of ARF GTPase-activating protein GIT1	GIT1	-3.71	0.0376
Dipeptidyl peptidase 1	CTSC	-3.70	0.0499
DNA-directed RNA polymerase II subunit RPB3	POLR2C	-3.68	0.0270
Chimera CSNK2B-LY6G5B splicing isoform 991	CSNK2B	-3.68	0.0394
Cation-independent mannose-6-phosphate receptor	IGF2R	-3.68	0.0940
ATPase ASNA1	ASNA1	-3.67	0.0028
H/ACA ribonucleoprotein complex subunit 2	NHP2	-3.65	0.0335
Arfaptin-1	ARFIP1	-3.65	0.0502
Isoform 4 of Dynamin-3	DNM3	-3.65	0.0072
Ribonucleoprotein PTB-binding 1	RAVER1	-3.65	0.0058
Protein NipSnap homolog 2	GBAS	-3.60	0.0224
Isoform 2 of General vesicular transport factor p115	USO1	-3.60	0.0175
Vesicle-associated membrane protein-associated protein B/C	VAPB	-3.60	0.0058
Ras-related protein Rab-21	RAB21	-3.60	0.0080
60 kDa SS-A/Ro ribonucleoprotein	TROVE2	-3.59	0.0367
Epidermal growth factor receptor	EGFR	-3.59	0.0229
Zinc finger CCCH-type antiviral protein 1	ZC3HAV1	-3.57	0.0184
NADH dehydrogenase [ubiquinone] 1 alpha subcomplex subunit 5	NDUFA5	-3.55	0.0114
Isocitrate dehydrogenase [NAD] subunit alpha, mitochondrial	IDH3A	-3.51	0.0438
Isoform 4 of Alpha-actinin-1	ACTN1	-3.50	0.0370

Gene Description	Gene	log2ratio VP treated/control	p-value
Putative coiled-coil-helix-coiled-coil-helix domain-containing protein CHCHD	CHCHD2P9	-3.48	0.0147
Procollagen galactosyltransferase 1	COLGALT1	-3.46	0.0434
Isoform 2 of Isochorismatase domain-containing protein 2, mitochondrial	ISOC2	-3.43	0.0325
Adenylate kinase isoenzyme 1	AK1	-3.41	0.0463
Isoform 2 of Protein FAM98B	FAM98B	-3.41	0.0349
Nuclear inhibitor of protein phosphatase 1	PPP1R8	-3.41	0.0341
Isoform 2 of Protein ELYS	AHCTF1	-3.41	0.0341
N-acetylserotonin O-methyltransferase-like protein	ASMTL	-3.32	0.0213
Septin-6	SEPT6	-3.30	0.0143
Uncharacterized protein C19orf43	C19orf43	-3.27	0.0161
Pterin-4-alpha-carbinolamine dehydratase	PCBD1	-3.27	0.0132
Isoform 3 of Bcl-2-like protein 2	BCL2L2	-3.21	0.0743
Cysteine and glycine-rich protein 1	CSRP1	-3.18	0.0179
Dolichyl-diphosphooligosaccharide--protein glycosyltransferase subunit 2	RPN2	-3.18	0.0308
Signal transducer and activator of transcription 3	STAT3	-3.16	0.0696
Cytochrome c oxidase subunit 5A, mitochondrial	COX5A	-3.07	0.0161
MICOS complex subunit MIC19	CHCHD3	-3.03	0.0434
N(G),N(G)-dimethylarginine dimethylaminohydrolase 1	DDAH1	-3.02	0.0442
Coiled-coil domain-containing protein 124	CCDC124	-3.01	0.0028
Cytochrome b-c1 complex subunit 1, mitochondrial	UQCRC1	-2.96	0.0352
Isoform 2 of LIM and SH3 domain protein 1	LASP1	-2.89	0.0375
C-1-tetrahydrofolate synthase, cytoplasmic	MTHFD1	-2.88	0.0506
Fumarate hydratase, mitochondrial	FH	-2.84	0.0003
14-3-3 protein zeta/delta	YWHAZ	-2.70	0.0069
Alpha-actinin-4	ACTN4	-2.67	0.0438
Phosphatidylethanolamine-binding protein 1	PEBP1	-2.58	0.0042
Isoform B of Ras-related C3 botulinum toxin substrate 1	RAC1	-2.47	0.0018
Fascin	FSCN1	-2.46	0.0336
LIM domain and actin-binding protein 1	LIMA1	-2.44	0.0347
Ras-related protein Rab-1A	RAB1A	-2.42	0.0212
Mitotic checkpoint protein BUB3	BUB3	-2.40	0.0161
RNA-binding protein 4	RBM4	-2.39	0.0508
Isoform 4 of LIM domain and actin-binding protein 1	LIMA1	-2.37	0.0369
60S ribosomal protein L36a	RPL36A	-2.37	0.0095
60S ribosomal protein L23	RPL23	-2.33	0.0178
60S ribosomal protein L15	RPL15	-2.17	0.0314
Isocitrate dehydrogenase [NADP] cytoplasmic	IDH1	-2.04	0.0125
Low molecular weight phosphotyrosine protein phosphatase	ACP1	-2.01	0.0502
Isoform 4 of Elongation factor 1-delta	EEF1D	-2.00	0.0390

Table S5: Proteomic Analysis of VP treated GBM Gliomaspheres. GBM301, GBM2 (EGFRvIII), and GBM1219 (EGFR wild-type) GSCs were treated with verteporfin (VP) for 6 hours and were subjected to label-free total proteomic profiling according to published protocols (1, 2). The table shows proteins that decreased an average 2-fold or more in protein levels in VP treated GSCs compared to control GSCs in the three GSC cell cultures profiled. The log2ratio values shown are averages for all three cell cultures profiled. The p-values shown represent multiple t tests for peptide-to-spectrum (PSM) matches for each protein in all three VP-treated GSCs compared to control GSCs. Proteins that showed different levels between control and VP treated samples with a p-value of .05 or less are listed in the table. Additional proteins with p-values greater than .05 for which we have documented protein level reductions by western blot (STAT3, IGF2R, BCL2L2) are also listed. Proteins with low abundance (1-2 PSMs) in control samples were excluded from analysis. Core signaling proteins are highlighted in yellow and and core metabolic and mitochondrial proteins uncovered by bioinformatic pathway analysis (see Table S5) are highlighted in blue. A total of different 5482 proteins were identified in our profiles.

1. Seyfried, N. T., E. B. Dammer, V. Swarup, D. Nandakumar, D. M. Duong, L. Yin, Q. Deng, T. Nguyen, C. M. Hales, T. Wingo, J. Glass, M. Gearing, M. Thambisetty, J. C. Troncoso, D. H. Geschwind, J. J. Lah and A. I. Levey (2017). "A Multi-network Approach Identifies Protein-Specific Co-expression in Asymptomatic and Symptomatic Alzheimer's Disease." Cell Systems 4(1): 60-72.e64.
2. Wingo, T. S., D. M. Duong, M. Zhou, E. B. Dammer, H. Wu, D. J. Cutler, J. J. Lah, A. I. Levey and N. T. Seyfried (2017). "Integrating Next-Generation Genomic Sequencing and Mass Spectrometry to Estimate Allele-Specific Protein Abundance in Human Brain." Journal of Proteome Research 16(9): 3336-3347.

Pathway ID	Pathway Name	Source	p-Value	FDR B&H	FDR B&Y	Bonferroni	Genes from Input	Genes in Annotation
1270125	Citric acid cycle (TCA cycle)	BioSystems: REACTOME	5.35E-10	3.49E-07	2.78E-06	8.51E-07	8	19
1270122	Pyruvate metabolism and Citric Acid (TCA) cycle	BioSystems: REACTOME	6.60E-10	3.49E-07	2.78E-06	1.05E-06	11	49
1270121	The citric acid (TCA) cycle and respiratory electron transport	BioSystems: REACTOME	1.25E-09	3.92E-07	3.11E-06	1.99E-06	18	171
82927	Citrate cycle (TCA cycle)	BioSystems: KEGG	1.48E-09	3.92E-07	3.11E-06	2.35E-06	9	30
132956	Metabolic pathways	BioSystems: KEGG	1.02E-07	1.82E-05	1.45E-04	1.62E-04	49	1272
814926	Carbon metabolism	BioSystems: KEGG	1.03E-07	1.82E-05	1.45E-04	1.64E-04	13	114
1269688	Processing of Capped Intron-Containing Pre-mRNA	BioSystems: REACTOME	4.08E-07	4.99E-05	3.96E-04	6.48E-04	18	248
413347	Citrate cycle, first carbon oxidation, oxaloacetate	BioSystems: KEGG	6.28E-06	5.55E-04	4.41E-03	9.98E-03	4	8
1269695	Transport of Mature mRNAs Derived from Intronless Transcripts	BioSystems: REACTOME	1.25E-05	9.06E-04	7.20E-03	1.99E-02	7	45
1269114	Transport of Ribonucleoproteins into the Host Nucleus	BioSystems: REACTOME	1.45E-05	9.20E-04	7.31E-03	2.30E-02	6	31
1269922	Regulation of Glucokinase by Glucokinase Regulatory Protein	BioSystems: REACTOME	1.45E-05	9.20E-04	7.31E-03	2.30E-02	6	31
1339112	SUMOylation of RNA binding proteins	BioSystems: REACTOME	1.95E-05	1.10E-03	8.77E-03	3.09E-02	7	48
868084	Fatty acid metabolism	BioSystems: KEGG	1.95E-05	1.10E-03	8.77E-03	3.09E-02	7	48
1269697	Transport of the SLBP independent Mature mRNA	BioSystems: REACTOME	2.53E-05	1.26E-03	9.98E-03	4.02E-02	6	34
1269085	Rev-mediated nuclear export of HIV RNA	BioSystems: REACTOME	2.53E-05	1.26E-03	9.98E-03	4.02E-02	6	34
1269817	Nuclear Pore Complex (NPC) Disassembly	BioSystems: REACTOME	3.01E-05	1.41E-03	1.12E-02	4.78E-02	6	35
1269696	Transport of the SLBP Dependant Mature mRNA	BioSystems: REACTOME	3.01E-05	1.41E-03	1.12E-02	4.78E-02	6	35
1269877	Membrane Trafficking	BioSystems: REACTOME	3.15E-05	1.43E-03	1.14E-02	5.00E-02	26	614
83070	Adherens junction	BioSystems: KEGG	3.79E-05	1.59E-03	1.26E-02	6.02E-02	8	72
1269876	Vesicle-mediated transport	BioSystems: REACTOME	4.01E-05	1.63E-03	1.30E-02	6.36E-02	27	660
137918	Stabilization and expansion of the E-cadherin adherens junction	BioSystems: Pathway Interaction Database	6.61E-05	2.50E-03	1.99E-02	1.05E-01	6	40
413348	Citrate cycle, second carbon oxidation, 2-oxoglutarate	BioSystems: KEGG	8.26E-05	2.95E-03	2.34E-02	1.31E-01	4	14
1270128	Respiratory electron transport	BioSystems: REACTOME	8.49E-05	2.95E-03	2.34E-02	1.35E-01	9	103

Table S6. Pathway analysis of proteins downregulated in GBM cells by short-term VP treatment. Proteins that showed a 2-fold or more reduction upon 8 hours of VP treatment were identified by proteomic profiling of whole gliomaspheres (see Supplemental Table 3). The pathways over-represented among these proteins were identified using ToppGene (https://toppgene.cchmc.org/enrichment.jsp). Constituent proteins for each named pathway are provided in the links in the 'Proteins from Input' column.